Supplemental Appendix for

PIAS1 modulates striatal transcription, DNA damage repair, and SUMOylation with relevance to Huntington's disease

Authors: Eva L. Morozko[1]*, Charlene Smith-Geater[2]*, Alejandro Mas Monteys[3], Subrata Pradhan[4], Ryan G. Lim[5], Peter Langfelder[6], Marketta Kachemov[1], Austin Hill[7], Jennifer T. Stocksdale[1], Pieter R. Cullis[8, 9], Jie Wu[11], Joseph Ochaba[1], Ricardo Miramontes[5], Anirban Chakraborty[12], Tapas K. Hazra[12], Alice Lau[2], Sophie St-cyr[3], Iliana Orellana[13], Lexi Kopan[2], Keona Q. Wang[2], Sylvia Yeung[5], Blair R. Leavitt[10], Jack C. Reidling[5], X. William Yang[14], Joan S. Steffan[2, 5], Beverly L. Davidson[3, 15]#, Partha S. Sarkar[4, 16]#, Leslie M. Thompson[1, 2, 5, 11,13]#

Corresponding Author: Leslie M. Thompson
Email: lmthomps@uci.edu

This PDF file includes:

Supplementary Results

We evaluated open field, accelerating rotarod and body weight in zQ175 treated mice as described (1). In addition, a running wheel task (2) was used to assess motor deficits in presymptomatic Pias1 KD animals.

Symptomatic

Behavior: For open field task at 12.5 Mo, no significant differences were detected between groups for distance traveled or velocity (**SI Appendix, Figure S2A**). This data is consistent with the lack of a genotype effect in the presymptomatic cohort assessed with this task at 12.5 Mo and as observed previously for these animals (1). No differences were detected for males or females for percent of time in center separately but combined, animals showed a significant difference, suggesting that this cohort of zQ175 mice may have had increased anxiety ($F_{2, 44} = 3.380$, $p<0.05$, **SI Appendix, Figure S2A**). However, post-hoc analysis failed to reveal the source of significance.

To assess additional deficits in motor movements, accelerating Rotarod task was performed at 9.5 and 12.5 Mo (**SI Appendix, Figure S2B**). At 9.5 Mo, zQ175 animals had a significant decrease in latency to fall that was primarily observed in the females only as males alone did not show any significant difference in latency to fall between the groups (**SI Appendix, Dataset S1**). Pias1 KD had no effect on latency to fall at 9.5 Mo. At 12.5 Mo, no differences in latency to fall were detected for males and females separately, but combined showed a significant difference suggesting a slight decrease in latency to fall for zQ175 mice (Combined: $F_{2, 43} = 3.576$, $p<0.05$). However, post-hoc analysis failed to show significance between groups with combined animals further suggesting that miPias1.3 treatment did not affect behavioral readouts in zQ175 mice (**SI Appendix, Figure S2B**).

Body weight was also recorded for these animals and assessed separately due to the previously observed differences based on sex in these animals (1). Males did not show any differences in body weight at 12.5 Mo even though decreased body weight is typical in zQ175 mice at this age (1). For females, 1-way ANOVA suggested a significant genotype effect indicating decreased body weight ($F_{2, 24} = 4.226$, $p<0.05$) but with post-hoc analysis again failing to reveal significance (**SI Appendix, Figure S2C**). Symptomatic Pias1 KD did not affect body weights. Taken together,

behavioral data suggest that symptomatic miPias1.3 treatment does not affect behavioral readouts in zQ175 mice.

Biochemistry: Soluble/Insoluble fractionation was used (**SI Appendix, Figure S4**) to determine Pias1 protein levels and formation of insoluble HMW mHTT, a molecular readout modulated in cell culture and R6/2 mice by Pias1 (3). At 13.5 Mo. Pias1 did not show aberrant accumulation in the Insoluble fraction as observed previously in R6/2 mice (4), nor was insoluble Pias1 altered (Females: $F_{2, 11} = 3.262$, $p>0.05$; Males: $F_{2, 9} = 0.730$, $p>0.05$, **SI Appendix, Figure S4B, E**). HMW mHTT was not altered in symptomatic miPias1.3-treated animals (Females: $p>0.05$, males: $p>0.05$). A significant reduction of Pias1 was observed in the Soluble fraction in females only (**SI Appendix, Figure S4E, F**, Females: $F_{2,11}=14.510$, $p<0.001$; Males: $F_{2, 9} = 1.165$, $p>0.05$).

A decline in mHTT protein levels was previously associated with disease progression in knockin HD mice (5). To determine if Pias1 KD affected this genotype-associated decline, soluble, full-length HTT (FL HTT) protein was quantified using D7F7 antibody. While significantly lower levels of soluble FL HTT were observed in zQ175 mice, miPias1.3 treatment had no effect in either females ($F_{2, 11} = 19.830$, $p<0.001$) or males ($F_{2, 9} = 12.060$, $p<0.01$, **SI Appendix, Figure S4C, F**), suggesting that Pias1 is not modulating age-associated decline of mHTT protein (5). Taken together, targeting Pias1 symptomatically in the zQ175 mice did not affect behavioral deficits or accumulation of insoluble mHTT species.

Presymptomatic KD (13.5-month old sacrifice)

Open field task: To assess motor deficits and anxiety, the open field task was performed at 7.5 and 12.5 Mo and analyzed by Ethovision™ video tracking software. Deficits in total distance traveled were previously reported at 7.5 Mo for zQ175 heterozygous mice (1). At 7.5 Mo, both zQ175 males and females had significantly less distance traveled with slower velocity. This was retained analyzing both sexes combined with no effect of Pias1 KD treatment observed (**SI Appendix, Dataset S1**, **Figure S3A).** These data support a clear zQ175 motor deficit but miPias1.3 treatment had no effect on motor behavior in these animals at 7.5 Mo. No effects were observed for percent of time spent in center zone for any group indicating a lack of anxiety phenotype in these animals that was not affected by miPias1.3 treatment. At 12.5 Mo, zQ175 motor deficits were no longer

observed and there was no miPias1.3 treatment effect (**SI Appendix, Figure S3**). No anxiety phenotype was observed for percent time spent in center zone. Loss of genotype effect is common in these animals at later ages (1) and overall Pias1 KD did not affect these behavioral readouts.

Rotarod: Rotarod detects genotype differences starting at 7.5 Mo in zQ175 mice (1). No overt miPias1.3 treatment effects were observed for either males or females in latency to fall in this study (**SI Appendix, Figure S3**C, **Dataset S1**). Specifically assessing latency to fall at 9.5 Mo both males and females showed a significant genotype effect that was retained when combined, indicating that zQ175 mice had a decreased latency to fall (**SI Appendix, Figure S3**C). No treatment effect was observed for either sex when analyzed separately or for males and females combined. Interestingly, at 12.5 Mo, male heterozygote animals with miPias1.3 treatment may have had a slight rescue in latency to fall as observed by a significant interaction detected by 2-way ANOVA (Interaction, $F_{1, 26} = 4.473$, $p<0.05$). This effect was not observed in females and only the genotype effect was observed analyzing the combined group (Genotype: $F_{1, 53} = 9.958$, $p<0.01$, **SI Appendix, Figure S3**C), further suggesting that miPias1.3 treatment does not affect motor phenotypes in these animals.

Body weight: zQ175 heterozygous animals reliably show decreased body weight (1). Male zQ175 animals had significantly lower body weights than their WT counterparts with Pias1 KD not altering this genotype effect (**SI Appendix, Dataset S1**, **Figure S3D**). In female animals, only a decrease in weight was observed for miPias1.3 treated zQ175 animals, but with no significant treatment effect (Treatment: $F_{1, 23} = 2.592$, $p>0.05$). Overall, males showed a significant genotype effect while female zQ175 animals did not show a genotype effect but may have decreased body weight with Pias1 KD.

Running Wheel: The running wheel task allows for uninterrupted, voluntary assessment of motor function and motor learning (2). Therefore, males were assessed at 9 Mo for two weeks. Females were not analyzed due to the influence of estrus cycle on running wheel activity (2). Running wheel data trends suggest a promotion of motor deficits in mice treated with miPias1.3 in both WT and zQ175 mice compared to miSafe-treated controls, but with no significant treatment effect over time (Treatment: $F_{3, 15} = 3.257$, $p>0.05$, **SI Appendix, Figure S3E**). Overall, miPias1.3 treated

zQ175 mice performed worse throughout the task and WT animals with miPias1.3 treatment showed a significant reduction in wheel-usage at days 3 and 5, suggesting a negative impact on this task with miPias1.3 treatment on WT and HD mice at this age (**SI Appendix, Figure S3E**).

The running wheel task can also be used to assess motor learning based on the slope of mean running between days 2 and 10 (2). Using this analysis, no differences in motor learning were observed between our groups (Genotype, $F_{1, 15} = 0.510$, $p>0.05$; Treatment, $F_{1, 15} = 0.741$, $p>0.05$, **SI Appendix, Figure S3E**). Overall, running wheel data may suggest an exacerbation in motor deficits in zQ175 animals and a decreased usage effect in WT animals with miPias1.3 presymptomatic treatment when assessed at 9 Mo, with no effect on motor learning.

Biochemistry: In males, no differences in Pias1 protein levels were detected in either WT or zQ175 mice in either the Insoluble (Treatment: $F_{1, 8} = 3.709$, $p>0.05$, Genotype: $F_{1, 8} = 0.069$, $p>0.05$) fraction or Soluble (Treatment: $F_{1, 8} = 0.533$, $p>0.05$, Genotype: $F_{1, 8} = 0.104$, $p>0.05$) fraction (**SI Appendix, Figure S5B**). In zQ175 males, HMW mHTT was not modulated with miPias1.3 treatment. FL-HTT was again significantly lower in zQ175 males at this time point compared to WT ($F_{1, 8} = 39.600$, $p<0.001$), but no miPias1.3 treatment effect was observed ($F_{1, 8} = 0.935$, $p>0.05$, **SI Appendix, Figure S5B, C**), suggesting that presymptomatic KD of Pias1 did not impact age-associated decline of mHTT. In female animals, Pias1 protein was also not significantly reduced in either WT or zQ175 mice for either the Insoluble ($F_{1, 10} = 4.464$, $p>0.05$) or Soluble fractions ($F_{1, 10} = 2.512$, $p>0.05$, **SI Appendix,Figure S5E, F**), however, insoluble HMW mHTT showed a higher intensity in females with miPias1.3 treatment ($p<0.05$). No treatment effect was observed on levels of soluble, FL HTT ($F_{1, 10} = 1.879$, $p>0.05$) which was also reduced in zQ175 female mice ($F_{1, 10} = 43.570$, $p<0.0001$). Therefore, Pias1 KD appears to have a selective influence on the accumulation of insoluble, HMW mHTT in females only by 13.5 Mo.

Presymptomatic KD (8-month old sacrifice)

Behavior: For this group, only a significant genotype effect in percent time spent in the center was observed for the Open Field task at 7.5 Mo (Genotype: $F_{1, 34} = 13.09$, $p<0.001$, **SI Appendix, Figure S6A).** Bodyweight was recorded and assessed as in previous cohort until 8 Mo. No

differences in weight gain were detected for either genotype or treatment by 8 Mo (**SI Appendix, Figure S6B**). However, at 8 Mo, zQ175 mice only exhibit minor deficits in body weight (1). It is possible that this cohort of animals had not begun showing detectable genotype effects with this analysis by time of sacrifice.

The running wheel apparatus has a finite number of animals that can be tested at a time due to single housing. Therefore, groups of male mice were of comparable size to the cohort assessed at 9 Mo and data was similarly processed (**SI Appendix, Figure S6C**). In contrast to mice tested at 9 Mo, which showed some additional impairment in this task with Pias1KD, at this earlier time point, KD increased running wheel usage. Specifically, a significant treatment effect (Treatment: $F_{3, 12} = 3.526$, $p<0.05$) was observed with WT animals treated with miPias1.3 showing an apparent increase in usage of the running wheel over time compared to WT control treated animals. A similar trend was observed between zQ175 miSafe and miPias1.3 treated animals over time. No differences were detected in motor learning (Genotype: $F_{1, 12} = 1.339$, $p>0.05$; Treatment, $F_{1, 12} = 4.663$, $p>0.05$). Overall, data suggests that miPias1.3 treatment led to increased usage of the running wheel and increased motor capabilities in at least WT animals and potentially zQ175 animals at this time point (7 months, **SI Appendix, Figure S6C**). Therefore, miPias1.3 presymptomatic treatment may have differential effects on behavior during different stages of disease pathogenesis.

Biochemistry: Pias1 protein levels were significantly reduced in the Soluble fraction in both WT and zQ175 males treated with miPias1.3 (Treatment: $F_{1, 10} = 76.120$, $p<0.0001$ **SI Appendix, Figure S7A**). Insoluble Pias1 levels also showed a significant treatment effect between control WT animals and miPias1.3 treated zQ175 ($F_{1, 10} = 12.920$, $p<0.01$, **SI Appendix, Figure S7C**). Levels of insoluble Pias1 were not elevated in untreated zQ175 animals at this age, similar to 13.5-month old animals, supporting a different baseline from R6/2 mice in these animals. However, this reduction of Pias1 still did not affect formation of insoluble HMW mHTT accumulated species ($p>0.05$). A modest treatment effect on the reduced FL HTT in zQ175 mice (Genotype: $F_{1, 10} = 31.990$, $p<0.0001$) was observed with miPias1.3 treatment (Treatment: $F_{1, 10} = 7.564$, $p<0.05$). Striata from female mice were also assessed (**SI Appendix, Figure S7B**). In the Soluble fraction, a significant treatment effect was observed ($F1, 10 = 14.72$, $p<0.01$) but post-hoc analysis failed

to reveal source of significance due to a large amount of variability in zQ175 miPias1.3 treated samples. This variability inversely corresponded to levels of detected GFP, suggesting that lack of significant reduction was due to insufficient viral transduction (**SI Appendix, Figure S7B**). Excluding zQ175 KD sample with the least amount of GFP, a significant reduction in Pias1 is observed in both WT and zQ175 treated animals ($F_{1, 9} = 26.90$, $p<0.001$). Insoluble Pias1 levels also showed a significant treatment effect with ($F_{1, 10} = 9.124$, $p<0.05$) and without ($F_{1, 9} = 6.27$, $p<0.05$) low expressing GFP KD sample, but with no post-hoc significance detected. This suggests a possible fraction shift with miPias1.3 treatment in females. Levels of insoluble Pias1 were still not elevated at baseline in zQ175 mice compared to WT ($F_{1, 10} = 0.284$, $p>0.05$). Levels of HMW mHTT were still not affected with miPias1.3 treatment ($p>0.05$). Only a significant genotype effect was detected for FL HTT (All samples: $F_{1, 10} = 126.5$, $p<0.0001$, KD only samples: $F_{1, 9} = 152.10$, $p<0.0001$), suggesting that Pias1 consistently does not modulate levels of this huntingtin species in zQ175 mice.

Bulk mRNAseq of females, presymptomatic treatment assessed at 13.5 months of age

Four conditions were assessed for female mice at 13.5 Mo: WT miSafe, WT miPias1.3, Het zQ175 miSafe, and Het zQ175 miPias1.3, with three mice each per condition. PCA on the top 500 genes showed separation between genotype but not by treatment (**SI Appendix, Figure S10A**).

DEseq2 analysis to determine DEGs (6) revealed only 157 disease-associated DEGs between WT and zQ175 miSafe treated animals. 194 DEGs were observed in WT animals with miPias1.3 treatment, and 57 DEGs observed in zQ175 with miPias1.3 treatment (**SI Appendix, Dataset S2, Figure S10B**). Compared to male mice at this age, an overlap of only 3 shared DEGs was observed, with Pias1 being down-regulated in both (**SI Appendix, Figure S10C**). Further, only 4 DEGs were in common between genotypes in females at this age (**SI Appendix, Figure S10D**) suggesting differential impact of Pias1 KD between genotypes in female mice. Supporting this, GO enrichment revealed differential biological processes for WT compared to zQ175 animals with Pias1 KD (**SI Appendix, Dataset S3**, **Figure S10E, F**) as well as a significant negative concordance between males and females with miPias1.3 treatment from this cohort as seen by a scatter plot of Z scores calculated using the log2FC from each dataset (**SI Appendix, Figure**

S10G). However, comparison with previously published allelic series showed significant concordance, suggesting a consistent molecular genotype effect (**SI Appendix, Figure S10H**).

Generation of PIAS1 heterozygous null iPSC lines using CRISPR/CAS9 genome editing

Clones were generated by targeting exon 2 of the PIAS1 locus (**SI Appendix, Figure S16A**). Several clones were validated for in-dels by genomic DNA sequencing and the specific mutation shown to be a deletion in the 33Q and an insertion in the 66Q iPSC clones generating two heterozygote PIAS1 KD lines (**SI Appendix, Figure S16B, C**); both produced shortened transcripts that resulted in significantly reduced levels of PIAS1 protein product as assessed by western blot in iPSCs ($p<0.05$, **SI Appendix, Figure S16D, E**). iPSC clones were assessed by immunofluorescence for pluripotency (**SI Appendix, Figure S16F, G**) and lines had normal karyotype (46XX-CgH array at Cell Linge Genetics, WI, USA). Next, the capacity to differentiate into neurons was assessed using a 37-day protocol to derive MSNs (**SI Appendix, Figure S17A** (7)). Cell lines showed comparable DARPP32 and BCL-11B co-staining, and MAP-2 staining at the end of differentiation indicating successful differentiation (**SI Appendix, Figure S17B, C**), and revealing that PIAS1 reduction does not impact differentiation into neurons.

Supplementary Discussion

Unexpectedly, Pias1 KD did not show significant or consistent effects or alter behavior in the zQ175 mice, unlike what we previously observed in the R6/2 model (4). This may be due to the subtle behavioral phenotype observed for zQ175 mice that can be challenging to measure and in fact even lost over time (8, 9). Supporting this, studies have reported subtle or no behavioral alterations while still having robust molecular changes utilizing zQ175 mice as a model for HD (10, 11).

We also do not observe robust changes in accumulation of HMW mHTT species in the presence of Pias1 KD as in R6/2 mice. However, there was a significant accumulation of insoluble Pias1 in R6/2 striatum, that we do not observe in zQ175 striatum (4). In R6/2 mice, miPias1.3 treatment specifically reduced insoluble Pias1 protein levels, in parallel with reduction of insoluble HMW mHTT (4), whereas in zQ175 mice, reduction of Pias1 is confined to the Soluble fraction. Therefore, it is possible that zQ175 mice display a differential baseline of Pias1 activity and

homeostasis reflected in its localization compared to the R6/2 mouse model. This difference may explain why insoluble Pias1 remained unchanged in zQ175 mice with KD and in part, may account for the differences in effects on behavior and HMW mHTT accumulation in this study. Future studies will investigate the functional contributions of insoluble versus soluble Pias1 on molecular pathways and whether the transition between fractions is a reflection of the pathogenic process that impacts early versus later neuropathology

We observed differences based on sex in genes affected by Pias1 KD, and opposite effects of Pias1 KD on HMW mHTT accumulation in female mice at 13.5 Mo compared to males; these differences remain to be explored. A direct influence of estrogen on gene expression is possible for BDNF, ARC, and BCL2L2 (12-14) and BDNF contains a putative estrogen response element within its promoter (15). However, there is a limited amount of evidence for hormone transcription factor binding in human and mammalian brains (16) and while sex-specific fluctuations in gene expression may exist, recent transcriptomic profiling in multiple human brain regions including the caudate and putamen did not identify sex-specific expression bias for BDNF, ARC, NEUROD1, NEUROD2, or BCL2L2 (17). It is noteworthy that the vast majority of transcriptomic and behavioral studies in R6/2 mice have been carried out in males, and previous transcriptional profiling in zQ175 mice removed sex-associated variation (18). Of interest, transcriptional analysis of LNP-mediated PIAS1 KD predicted activation of β-estradiol and estrogen receptor 1 (ESR1) in control and HD iPSC-derived neurons (**Figure 4F**), suggesting that PIAS1 may have a sex-dependent function. This hypothesis is the basis for future work.

Supplemental Experimental Procedures

zQ175 knockin mice

CAG repeat sizing of genomic DNA harvested from tails was performed by Laragen. Male and female littermates were subjected to bilateral intrastriatal injections to deliver treatment at either 2.5 (presymptomatic) or 7.5 (symptomatic) Mo. Littermates of the same sex were randomly assigned to experimental groups and were group housed, mixed genotype, for majority of experiments with the exception of male mice subjected to running wheel task which were single-housed during and after completion of running wheel assessment. Experiments were carried out in strict accordance with the Guide for the Care and Use of Laboratory Animals of the NIH and an

approved animal research protocol by the Institutional Animal Care and Use Committee (IACUC) at the University of California, Irvine. Animals were humanely euthanized by an over-dose injection of Euthasol followed by whole body perfusion with 1x-PBS and decapitation.

iPSC derivation and maintenance

HD and non-disease repeat iPSCs were generated and characterized as described (7, 19). iPSCs [(CS71iCTR20n6, XX, age of sampling (AOS) 61, CS83iCTR33n1, XX, AOS 21; CS25iCTR18n6, XY, AOS 76, CS14iCTR28n6, XX, AOS unknown, CS02iHD66n4, XX, AOS 20, CS81iHD71n3, XX, AOS 20, (7) and CS09iHD109n4, XX, AOS 9 (19)] were maintained in mTESR1 (Stem Cell Technologies) on hESC-qualified Matrigel (Fisher Scientific) at 37^{o}C at 5% CO_2, then passaged using Versene (Gibco) at a ratio of 1:3 to 1:6, depending on confluency. Colonies were cryopreserved in CryoStor CS10.

HeLa and SH-SY5Y cell culture

HeLa cells were cultured in Dulbecco's Modified Eagle Medium (DMEM) with High glucose supplemented to 10% fetal bovine serum (FBS) at 37°C, 5% CO_2 and passaged at 95% confluency. $3.0x10^5$ cells/well were plated in 6-well dishes and transfected with cDNA plasmid and/or siRNA (PIAS1 knock-down: PIAS1 siRNA sense sequence: AUCACCUCACUUGUCCGACUGUUU, Dharmacon) using Lipofectamine 2000 (Life Technologies 11668019) at ~60% confluency. Media was changed 24 hours post transfection. Cells were harvested 44 hours post transfection. Transfected plasmids: PIAS1, His-SUMO-1 and SUMO-2 were used as previously described (20) and Myc-PNKP construct described below. Human neuroblastoma SH-SY5Y cells were purchased from American Type Culture Collection (ATCC; Catalogue number CRL-2266) and cultured in Dulbecco's Modified Eagles Medium (DMEM) with high glucose and containing 15% fetal bovine serum (FBS), and 1% penicillin-streptomycin in CO_2 incubator at 37°C.

Surgery

At 2.5 Mo or 7.5 Mo, cohorts of zQ175 mice were anesthetized using isoflurane and underwent bilateral intrastriatal injections using a dual injection stereotaxic apparatus (coordinates 0.01 mm caudal to bregma, 0.2 mm right/left of midline, 0.345 pocket to 0.325 mm ventral to pial surface) as previous (4). 5 µl of AAV2/1 virus containing miPias1.3 CMVeGFP or miSafe CMVeGFP at

~ 3e12 vg/ml was injected using a Hamilton syringe at a rate of 0.5 µl/min. Syringe was left in place for 5 minutes after each injection to ensure complete ejection of viral solution into brain region. Incisions were sutured and animals were allowed to fully recover on a heating pad then monitored daily for 1 week prior to beginning behavioral analysis.

Behavioral Paradigms

For zQ175 Pias1 presymptomatic KD cohorts, animal body weights were measured weekly over the course of the studies. Motor deficits were assessed by a running wheel (0297-0521-D60; Columbus Instruments) at 7 or 9 Mo depending on date of sacrifice. Mice had free access to running wheel usage that was constantly monitored over two weeks and collected in three-minute bins using Multi-Device System software 24-Channel Version 1.55 (160640; Columbus Instruments). Data from dark phase only was analyzed for significance over the two-week period. Motor learning was calculated as previously described (2). Briefly, slopes were calculated using formula $(Y_2-Y_1)/(X_2-X_1)$ where Y_2 is wheel usage per bin on night 10 and X_2 is 10 (night 10), and Y_1 is wheel usage per bin on night 2 with X_1 as 2.

The rotarod apparatus was used to measure fore and hind limb motor coordination and balance and mice were tested using an accelerating assay (Dual Species Economex Rota-Rod; 0207-003M; Columbus Instruments) at 9.5 and 12.5 Mo under blinded conditions. Animals were tested over two days with four trial runs each day consisting of 5-minute trial periods. Animals were acclimated to behavior room for 1 hour prior to testing. The first trial for each test day was used as a training trial and not used in final calculations. The latency to fall for the three final trials on day 2 of testing were averaged and analyzed for significance.

To assess anxiety and measure an additional motor task, animals were subjected to open field test at 7.5 Mo and 12.5 Mo when applicable. Animals were acclimated to behavior room for 1 hour prior to testing. Mice were allowed to explore an empty open field box for 5 minutes. Activity during these five minutes was recorded and analyzed using Ethovision™ Software that determines time spent in the center or on the periphery, average velocity and distance traveled over the 5 minute test period. Velocity and distance traveled during the open field trials were used as

measures of motor performance while percent time spent in center was used as a measure of anxiety.

Soluble/Insoluble Fractionation tissue lysis for protein quantification and Western Blot analysis

Flash frozen brain tissue was prepared as previous for Soluble/Insoluble fractionation (3, 4). Protein fractions were quantified using detergent compatible (DC) protein assay (Bio-Rad). Soluble protein lysates were resolved on 4-12% Bis-Tris Poly-Acrylamide gels and transferred onto either 0.45µM or 0.2µM nitrocellulose membrane depending on size of proteins of interest (smaller proteins on 0.2µM). Insoluble protein lysates were resolved on 3-8% Tris-Acetate Poly-Acrylamide gels and transferred onto 0.45µM nitrocellulose membrane. For LiCor assessed membranes, prior to blocking, total protein was assessed using Revert total protein stain (Li-Cor Biosciences 926-11016) and imaged using Odyssey CLx imager. Membranes were blocked in Intercept starting block (Li-Cor Biosciences 927-60010) for 1 hour prior to incubation in primary antibodies overnight at 4°C. Goat-anti-Rabbit secondary (IRDye 800CW or 680LR, LI-COR), goat-anti-Mouse IgG secondary (IRDye 800CW or 680LR, LI-COR), and donkey-anti-Goat (IRDye 800CW, LI-COR) were used to detect proteins at 1:10,000 dilutions and detected using a Li-Cor Odyssey CLx system. IR fluorescence imaging was used for quantitative analysis with detected protein levels normalized to Revert Li-Cor whole-protein stain prior to statistical analysis. Insoluble, HMW mHTT was quantified using 5492 antibody (Milipore MAB5492). Soluble, full-length HTT protein was quantified using D7F7 antibody (Cell signaling #5656S). Anti-PIAS1 (Cell signaling #3550S), anti-PNKP (Novus Biologicals NBP1-87257), and anti-GFP (Takara Bio, #632381) were also used.

RNA purification, mRNAseq and qPCR Analysis

For zQ175 mice, GFP+ micro-dissected flash frozen brain regions were homogenized in TRIzol reagent (Invitrogen) and RNA was extracted according to manufacturer's protocol. RNA was then purified using RNEasy Mini kit (QIAGEN). Residual DNA was removed by DNase treatment incorporated into the RNEasy protocol as per manufacturer's suggestion prior to qPCR or submitting for mRNAseq as previously described (21). Potential off-target genes for miPias1.3 were determined using siSPOTR as previously described (22, 23) with TPOTS score above 0.1

representing the potential for being real (**SI Appendix, Table S1**). For iPSC-derived neurons, RNA was extracted from day 37 cell pellets using Qiagen RNeasy kit and QIAshredders, 1 µg of RNA with Rin values >8 for each sample were utilized for library preparation and RNAseq as previously described (7). To confirm Pias1 knock-down in zQ175 mice, reverse transcription was performed using SuperScript 3 First-strand synthesis system according to manufacturer's protocol (Invitrogen, 18080085) from harvested and purified RNA. Both oligo (dT) and random hexamer primers were used in a 1:1 ratio. Final synthesized cDNA was diluted to 5ng/ul in DEPC treated water and stored at -20°C until use. For qPCR, technical triplicates for each individual animal were used to determine mean CT values. DeltaCT was calculated by subtracting mean CT of Eif4a2, a house-keeping gene which does not have a genotype effect in zQ175 mice (9), from mean CT of target gene per animal. Primers used for qPCR are listed in **SI Appendix Table S2**.

Differential expression analysis of combined data

mRNAseq datasets from this study were compared to previously published allelic series transcriptional profiles (18). Genes were first filtered for at least 1cpm in at least ¼ of the total number of samples. To make DE analysis more robust against potential outlier measurements (counts) that may remain even after outlier sample removal, we defined individual observation weights designed to downweigh potential outliers as described in (24) and (25). DE analysis was carried out using DESeq2 (6) version 1.22.2 with default arguments except for disabling outlier replacement and independent filtering. In the combined data analysis, batch was used as a covariate. Enrichment calculations were carried out using R package anRichment (https://horvath.genetics.ucla.edu/html/CoexpressionNetwork/GeneAnnotation/) that implements standard Fisher exact test and a multiple-testing correction across all query and refence gene sets.

iPSC neuronal differentiation

The iPSCs were cultured to 70% confluency then neuronal differentiation was started. At day 0 iPSC were washed with PBS (without Ca^{2+}/Mg^{2+}) and then switched into SLI medium (ADF supplemented with 2 mM Glutamax™, 2% B27 without vitamin A, 10 µM SB431542, 1 µM LDN 193189 and 1.5 µM IWR1). Daily media changes performed and at day 4, cells were passaged 1:2. To inhibit cell death upon dissociation, cells were pre-treated for 1 hour at 37ºC with 10 µM Y27632 dihydrochloride. Cells were washed with PBS (-Ca^{2+}/-Mg^{2+}) and dissociated using

Stempro Accutase (Life Technologies) at 37ºC for 5 minutes. Cells were re-plated in SLI medium containing 10 µM Y27632 dihydrochloride onto hESC-qualified Matrigel (Corning) and switched into medium without 10 µM Y27632 dihydrochloride on day 5. Cells were passaged again on day 8 in the same manner as above in a ratio of 1:2 and replated in LIA medium (ADF supplemented with 2 mM Glutamax™, 2% B27 without vitamin A, 0.2 µM LDN 193189, 1.5 µM IWR1 and 20 ng/ml Activin A) containing 10 µM Y27632 dihydrochloride. Medium changes were performed daily with LIA medium until day 16. Cells were dissociated as above and re-plated into SCM1 medium (ADF supplemented with 2 mM Glutamax™, 2% B27 supplement, 2 µM PD 0332991 (Tocris, USA), a CDK4/6 inhibitor, 10 µM DAPT (Tocris, USA), 10 ng/ml brain-derived neurotrophic factor (BDNF, Peprotech), 10 µM Forskolin, 3 µM CHIR 99021, 300 µM γ-amino butyric acid (GABA, all Tocris), supplemented with $CaCl_2$ to final concentration of 1.8 mM) and 200 µM Ascorbic acid (both Sigma-Aldrich) for neuronal differentiation on nitric acid (Fisher Scientific) washed borosilicate 12 mm glass coverslips (VWR) pre-treated with 100 µg/ml poly-D-lysine hydrobromide (Sigma Aldrich) and hESC-qualified Matrigel and plated at a density of 8 x 10^4 cells/cm^2. Half medium changes were performed on days 18 and 21. On day 23 medium was changed to SCM2 medium (1:1 ADF:Neurobasal A supplemented with 2 mM Glutamax™, 2% B27 supplement, 2 µM PD 0332991, 10 ng/ml BDNF, 3 µM CHIR 99021, 1.8 mM $CaCl_2$ and 200 µM Ascorbic acid). 50% media changes were then performed every 2-3 days until harvest at day 37.

iPSC CRISPR modification and validation of CRISPR clones

At 70% confluence, iPSCs (CS83iCTR33n1 and CS02iHD66n4) were pre-treated with 10 µM Y27632 dihydrochloride Rho kinase inhibitor for 1 hour to prevent cell death during single cell suspension. Cells were transfected with the CRISPR/CAS9 RNP complex and a pEF1α-puromycin plasmid to allow for selection of successfully transfected colonies. CRISPR-guide RNA CAS9 ribonucleic acid protein complex was made as follows: both guide RNAs, Alt-R CRISPR-CAS9 crRNA for targeting the PIAS1 locus and the Alt-R tracR RNA were mixed with Nucleic acid duplex buffer (all IDT Technologies) to a final concentration of 1 µM and heated to 95ºC for 5 minutes in a thermocycler and allowed to cool to room temperature. CAS9 protein (IDT) is diluted to 1 µM in Optimem medium (Life Technologies) and combined with the duplex in the following amounts per transfection 2.4 µl of Alt-R Guide RNA duplex, 1.7 µl of 1 µM CAS9 protein and

made up to 5 µl with PBS (with Ca^{2+} and Mg^{2+}) and incubated at room temperature for 20 minutes. Cells were prepared to a single cell suspension with Versene treatment for 5-10 minutes at 37ºC and then removed and replaced with mTESR1, cells were pipetted into a single cell suspension using a P1000 and collected by centrifuge at 200*xg* for 90 seconds. Cells were resuspended in 100 µl per transfection of Nucleofector solution II for hESC 1 µg of pmaxGFP plasmid (Lonza) and 1 µg of pEF1α-puro were added and 5 µl of the RNP complex were added to each cuvette with 100 µl of cell suspension. Cells were nucleofected using an AMAXA Nucleofector II device on program B-016. Cells were transferred to a 15 ml conical and mTESR1 supplemented with CloneR (Stem Cell Technologies) and 1 µM azidothymidine (AZT - Tocris) and 10 µM Y27632 dihydrochloride. Cells were plated between 4 wells of a 6-well plate on hESC-qualified Matrigel. One day after transfection, AZT was removed and cells were treated with 200 ng/ml puromycin for 48 hours with a daily media change. Clones were picked 24 hours after puromycin was removed by removing medium and treating cells for 30 seconds with Versene at 37ºC. Cells were placed in mTESR and colonies were picked using a P200 pipette tip and re-plated in a 12 well plate 1 colony per well in mTESR1 supplemented with CloneR. Cells were maintained in CloneR for 2 more days and then cells were maintained as above to collect enough cells for genomic DNA isolation and freezing back stocks. To validate genomic editing, iPSCs were pelleted and snap frozen in liquid nitrogen. Genomic DNA was extracted from the cells using the QIAGEN genomic DNA extraction kit (Qiagen). PCR across the region of interest containing potential in-dels was performed using the KAPA Hi-Fi PCR kit (KAPA Biosystems) following manufacturer's protocol. Formation of DNA heteroduplexes was performed by heating the double stranded DNA PCR product to 98ºC and then cooling 1ºC every 30 seconds to re-anneal DNA strands. Annealed products were then digested with the T7EI enzyme (NEB) and subsequently run on a 1% agarose TAE gel for assessment. Protein was harvested from frozen cell pellets of the clones using RIPA lysis buffer and run on a 4-12% Bis Tris polyacrylamide gel and transferred to 0.45 µm Nitrocellulose, blocked with Starting block (Invitrogen) and probed for PIAS1 (Cell signaling #3550S) and α-tubulin (Sigma T6079200). PCR products were cloned into the pGEM-T-easy cloning vector (Promega) and sequenced at Eurofins using T7 and SP6 enzymes. Sequences were analyzed on NCBI BLAST.

Immunofluorescence and microscopy

Cells were fixed with 4% paraformaldehyde (Fisher Scientific) for 10 minutes at room temperature, then washed three times with PBS (Fisher Scientific). Cells were permeabilized with 0.3% Triton-X (Sigma Aldrich) in PBS for 10 minutes and then blocked with 2% goat serum 3% BSA (Gibco) in PBS for 1 hour at room temperature and then incubated in primary antibody overnight at 4ºC (anti-DARPP32, (1:200) Abcam ab40801, anti-CTIP2 (1:500) Abcam ab18465, anti-FOXP1 (1:1000) Abcam ab16645, anti-MAP2 (1:1000) Millipore MAB3418, anti-NANOG (1:500) Santa Cruz sc-33759, anti-SSEA4 (1:100) Stem Cell Technologies 60062, anti-SOX2 (1:500) Millipore AB5603, anti-OCT4 (1:500) Millipore MAB4401). Primary antibody was removed and cells washed three times with PBS and then incubated for 1 hour in secondary antibody in the dark at room temperature (Goat anti Mouse IgG (H+L) Secondary Antibody, Alexa Fluor 594 (1:1000) Thermo Fisher Scientific A-11032, Goat anti Rabbit IgG (H+L) Secondary Antibody, Alexa Fluor 594 (1:1000) Thermo Fisher Scientific A-11037, Goat anti Mouse IgG (H+L) Secondary Antibody, Alexa Fluor 488 (1:1000) Thermo Fisher Scientific A-11029, Goat anti Rabbit IgG (H+L) Secondary Antibody, Alexa Fluor 488 (1:1000) Thermo Fisher Scientific A-11034). Cells were washed with PBS for three times and then washed in PBS containing Hoechst 33342 (Sigma-Aldrich) for 10 minutes and then a final wash in PBS. Coverslips were mounted with Fluoromount-G® (Fisher Scientific) and allowed to dry. Images were acquired on a Nikon T-E fluorescent microscope

PNKP enzymatic activity measurements

Nuclear extracts from cells and mouse tissue were prepared using NE-PER Kit (Thermo Scientific, Cat# 78835) and the proteins were quantified by Pierce BCA Assay Kit (Cat# 23225). Purified mitochondria were isolated from cells and mouse tissue using Mitochondrial isolation Kit (Thermo Sientific, Cat# 89874). The isolated mitochondria were lysed using pipette tip (~20 strokes) with Mitochondrial extraction Buffer [50 mM Tris-HCl, 150 mM NaCl, 1mM EDTA, 1mM DTT, 1% Triton X100, 10% glycerol, and protease inhibitors (Roche Applied Science, Germany) to extract mitochondrial protein. The mixture was centrifuged at 14000x g for 20 min, and the supernatant was taken as mitochondrial protein.

The 3'-phosphatase activity of PNKP in the nuclear extract (250–500 ng), mitochondrial extract, and purified recombinant His-tagged PNKP (25 fmol) was conducted as we described previously (26-29). Nuclear extracts for the 3' phosphatase assay was prepared following standard protocols from cells or mouse brains tissues (27, 30). A ^{32}P-labeled 3'-phosphate-containing 51-mer oligo substrate with a strand break in the middle (5 pmol) was incubated at 37°C for 15 min in buffer A (25 mM Tris-HCl, pH 7.5, 100 mM NaCl, 5 mM MgCl2, 1 mM DTT, 10% glycerol and 0.1 mg/ml acetylated BSA) with 5 pmol of unlabeled (cold) substrate. The reaction was stopped by adding buffer B (80% formamide, 10 mM NaOH) and the reaction products were electrophoresed on a 20% Urea-PAGE to measure the amount of 3' phosphate release from the radio-labeled substrate. The radioactive bands were visualized in PhosphorImager (GE Healthcare, USA). The data were represented as % of the phosphate release (% product) with the total radiolabeled substrate as 100.

Genomic DNA purification and Long-Amplification qPCR

Integrity of target genes was assessed using Long Amp Taq DNA polymerase (NEB, M0323L) to amplify products of >6kB. To ensure reaction remained within the linear range of amplification, cycle number and DNA concentration were standardized before final quantification to ensure the product remained within the linear amplification range (31).

For mouse genomic material, optimized conditions for each target gene were as follows: Neurod1 and Neurod2 (50 ng gDNA, 95°C for 1 min, 95°C for 25 s, 65°C for 25s, 65°C for 7.5 min. for 24 cycles, and 65°C for 7 min), Bdnf, Arc, and Bcl2l2 (60 ng gDNA, 95°C for 1 min, 95°C for 25 s, 65°C for 25s, 65°C for 7.5 min. for 25 cycles, and 65°C for 7 min). For normalization and to control for variability of genomic template, a short DNA amplicon was generated for each target gene using Q5® High-Fidelity Master Mix (NEB, M0492L). The same amount of input DNA from the same DNA aliquot and the same number of cycles were used for both short and long amplification reactions per gene. Short PCR conditions were 98°C for 1min., 98°C for 20 s, 65°C for 30 s, 72 for 40 s for 24 or 25 cycles (gene target optimized as above), and 72°C for 5 min.

For iPSC-derived MSN genomic and mitochondrial material, optimized conditions for all target gene was as follows: 94°C for 30 s (94°C for 30 s, 55–65°C for 30 s depending on the oligo annealing temperature, 65°C for 10 min) for 26 cycles and 65°C for 10 min. Each reaction used

50 ng of DNA template, and the LA-qPCRs for all studied genes used the same stock of diluted DNA samples to avoid amplification variations due to sample preparation. For mitochondrial DNA damage analysis, 5 ng template DNA was taken and the PCR was performed for 19 cycles. A small DNA fragment for each gene was amplified to normalize large fragment amplification. The PCR conditions were 98°C for 30 s, 66°C for 20 s, 72°C for 30 s for 26 cycles, and 72°C for 5 min. Short PCR used 50 ng of the template from the same DNA aliquot for nuclear genes and 5 ng DNA for mitochondrial genes. Products were then analyzed using agarose gel electrophoresis followed by densitometry analysis on ImageJ software. Primers used for LA-qPCR can be found in **SI Appendix Table S3**.

Construction of plasmid expressing Myc-tagged PNKP

Plasmid DNA clone carrying human PNKP cDNA was purchased from the Origene Technologies, USA (RC207551L1). The PNKP cDNA was PCR amplified and sub-cloned into plasmid pcDNA3.1-Hygro (+) (Invitrogen, USA). Synthetic DNA linkers encoding MYC-tag sequences were introduced at the N-terminal of PNKP to construct the final plasmid pcDNA-Myc-PNKP. The sequence integrity of the final recombinant plasmid was verified by sequencing, and appropriate expression of PNKP was verified by western blot and measuring PNKP activity.

Denaturing SUMOylation Assay

Denaturing SUMOylation assay was carried out as described with modifications (20). Specifically, HeLa cells were lysed under denaturing conditions in a buffer containing 6M guanidine HCl, 100 mM NaH2PO4 pH 7.8, and 10 mM Tris-HCl pH 7.8. Lysed cells were sonicated for 30 seconds at 40% amplitude. 5% lysis volume was removed for TCA precipitation. Remaining volume was used for His-purification under denaturing conditions by incubating lysed samples in lysis buffer together with His-isolation Dynabeads (Invitrogen, 10103D) for 1 hour at room temperature while rotating. Samples were washed twice in 8M urea with 100 mM NaH2PO4 pH 7.8, and 10 mM Tris-HCl pH 7.8, once in 8M urea with 100 mM NaH2PO4 pH 6.3, and 10 mM Tris-HCl pH 6.3 and once in 1X PBS. Beads were resuspended in loading buffer (1.6x loading dye, 1x reducing) and boiled for 10 minutes prior to western blot analysis. Whole-cell, 5% loading input was assessed using TCA precipitation. Sample 5% inputs in 6M guanidine lysis buffer were incubated in an equal volume of cold, 20% TCA and incubated on ice for 30 minutes. Precipitates were centrifuged

at 18,000xg for 15 minutes at 4°C. Supernatant was discarded and protein pellet was washed in ice-cold acetone followed by subsequent centrifugation at 18,000xg for 15 minutes at 4°C. Protein pellet was resuspended in loading buffer, pH was adjusted to basic with Tris-HCl pH 8, and samples were boiled for 10 minutes prior to western blot analysis. Protein was detected on western blot using anti-PNKP (Origene, AP16044PU-N), anti-Myc (Millipore, #05-419), anti-His (Qiagen, #34600), and anti-PIAS1(Cell Signaling, #3550S) antibodies.

Coimmunoprecipitation Assays

HeLa and differentiated iPSCs were lysed in buffer containing 20 mM Tris-HCl pH 7.5, 137 mM NaCl, 5 mM EDTA, 1% NP40 alternative, and 10% glycerol (Pierce Protease Inhibitor tablet, 0.2 mM NaF, 1:1000 dilution of inhibitor cocktails 2 & 3, 0.2 mM butyric acid, 5 mM nicotinamide, 1 mM PMSF, 1ug/uL aprotinin, 1ug/uL leupeptin, and 25 mM n-ethylmaleimide). HeLa cell Coimmunoprecipitations were carried out using 1 ug anti-Myc tag antibody (Millipore, #05-419) in lysis buffer without glycerol. Samples (400ug) were incubated for 1 hour together with anti-Myc tag antibody at 4°C while rotating. Dynabeads M280 (Invitrogen, 11201D) were then added to samples and rotated for 30 minutes at room temperature. Beads were washed 3x using a magnetic rack and lysis buffer without glycerol. For assessment of endogenous SUMOylated proteins in iPSCs, neuron pellets were lysed in lysis buffer (above) containing several deSUMOylation and phosphatase inhibitors (above). Pellets in lysis buffer were sonicated three times at 40% amplitude in 10 second intervals. A Bradford assay was then performed to assess protein concentration levels in lysates. Coimmunoprecipitation was carried out using an antibody against SUMO-2/3 (MBL M114-3). Protein G Dynabeads (Invitrogen, 10004D) were pre-washed three times with lysis buffer without glycerol (above) and 1 ug of SUMO2/3 antibody was pre-bound to 30 uL of magnetic Dynabeads Protein G (Invitrogen, 10004D) for 1 hour at 4°C while rotating in lysis buffer without glycerol. Replicates of each sample, omitting antibody, served as no-antibody negative controls. Following antibody-bead pre-incubation, 200 ug of lysate was added to each IP and incubated overnight at 4°C while rotating in 500 ul lysis buffer. The following day, samples were washed three times each with 500 ul lysis buffer without glycerol. Protein was eluted from the beads in 1x reducing loading dye and boiled for 5 minutes. SUMO elution was separated from the beads using a magnetic rack, collected, and analyzed by western blot. Specifically, cell lysates and immunoprecipitated proteins were assessed on 4-12% Bis-Tris PAGE

gels and transferred onto 0.45 µm PVDF-FL or PVDF. Membranes were assessed using LiCor Odyssey CLx imager as describe for Soluble/Insoluble fractionation. For assessment of PIAS1 KD and SUMOylated Co-immunoprecipitated proteins from iPSC derived neurons, membranes were assessed using chemiluminescence with either goat-anti-mouse (Jackson Laboratories #115035146) or goat-anti-rabbit (Thermo scientific # 31460) HRP-conjugated secondaries and SuperSignal™ West Pico substrate (Thermo Scientific #34580) captured on X-ray film.

Nuclear extracts from SH-SY5Y cells were isolated and treated with benzonase to remove DNA and RNA to avoid nucleic acid-mediated Co-IP. Specific target proteins were IP'd and washed extensively with cold Tris-buffered saline (50 mM Tris-HCl, pH 7.5, 200 mM NaCl) containing 1 mM EDTA, 1% Triton-X100, and 10% glycerol. The complexes were eluted from the beads with 25 mM Tris-HCl (pH 7.5) and 500 mM NaCl and analyzed by WB. WBs were performed according to standard procedure: elutions were run on SDS-PAGE and transferred onto Nitrocellulose Membrane. The membrane was blocked by 5% blocking solution (Skim milk) and incubated overnight with primary antibodies (1:1000 dilution) [mouse HTT (Millipore, MAB 2170), mouse RNA Polymerase 2A (Santa Cruz, Cat# sc-56767), Rabbit PIAS1 (Cell Signaling, Cat# 3550S), Rabbit PNKP (Novus, Cat# NBP1-87257). Proteins was detected with either mouse or rabbit or Protein A HRP (Cell Signaling, Cat# 12291S) antibodies and imaged using LI-COR Odyssey® Fc using Pierce ECL chemiluminescence kit (Cat # 32106) with 2-10 min exposure.

LNP Delivery

LNP-siRNA formulations were produced as described previously (32). Briefly, component lipids (MC3, DSPC, Chol, DiI and PEG-DMG) were combined in ethanol at a molar ratio of 50/10/38.3/0.2/1.5 (respectively) to a final concentration of 20 mM total lipid. siRNAs were dissolved in 25 mM sodium acetate pH 4 buffer. The two solutions were combined at a flow rate ratio of 3:1 (v/v) aqueous to organic phase using a T-junction mixer at a flow rate of 20mL/min (33). The resulting LNP suspension was dialysed against 1000-fold volumes of PBS pH 7.4 to neutralise the pH and remove the solvent. Subsequently, LNP-siRNA formulation was concentrated using Amicon centrifugal units (Millipore Sigma, Burlington, MA) to a final concentration of ~1 mg/mL siRNA. LNP-siRNA was added to cells at day 19 at a final concentration of 3.3µg/ml siRNA with 3µg/ml ApoE4 (final) during regular half media changes.

Luciferase siRNA sequence (sense: 5'-cuuAcGcuGAGuAcuucGAdTsdT-3', antisense: 5'-UCGAAGuACUcAGCGuAAGdTsdT-3', containing phosphorothioate linkages (indicated as the letter "s") between the 3'-dT overhangs and multiple 2'-OMe modifications (indicated by lower-case letters). PIAS1 siRNA sequence (sense: 5'- AUCACCUCACUUGUCCGACUGUUU-3', antisense: 5'- ACAGUCGGACAAGUGAGGUGAUUU-3').

Quantification and Statistical Analysis

Animal tissue data analyzed by Li-Cor Odyssey CLx Imager on western blot was quantified using ImageStudio software to determine IR-fluorescent intensity values. Relative target signal was normalized to total protein revert intensity signal. ECL analyzed western blots were quantified using ImageJ densitometry analysis and normalized to detected levels of α-Tubulin on the same blot. SUMO-modified species of PNKP were quantified using ImageStudio software and normalizing to abundance of 5% input from the same western and multiplying by 100. All data represented as mean ± SEM with a p value of $p<0.05$ considered statistically significant. Analyses were completed in GraphPad Prism™ software. Statistical analysis was completed of the delta CT (dCT) values obtained from qPCR reactions normalized to Eif4a2. For animal studies, "n" represents individual animals used for each assessment. For cell culture studies, "n" represents experimental replicates. All 2-way ANOVAs were followed by Tukey's multiple comparisons test. All 1-way ANOVAs were followed by Tukey's multiple comparisons test.

Data and Code Availability

The datasets generated during this study are available at GEO, accession number GSE162349. Original/source data for allelic series mRNA-seq comparison in the paper is available online at 10.1038/nn.4256 and available through HDinHD (https://www.hdinhd.org).

Supplemental Figures and Legends

Supplemental Figure S1

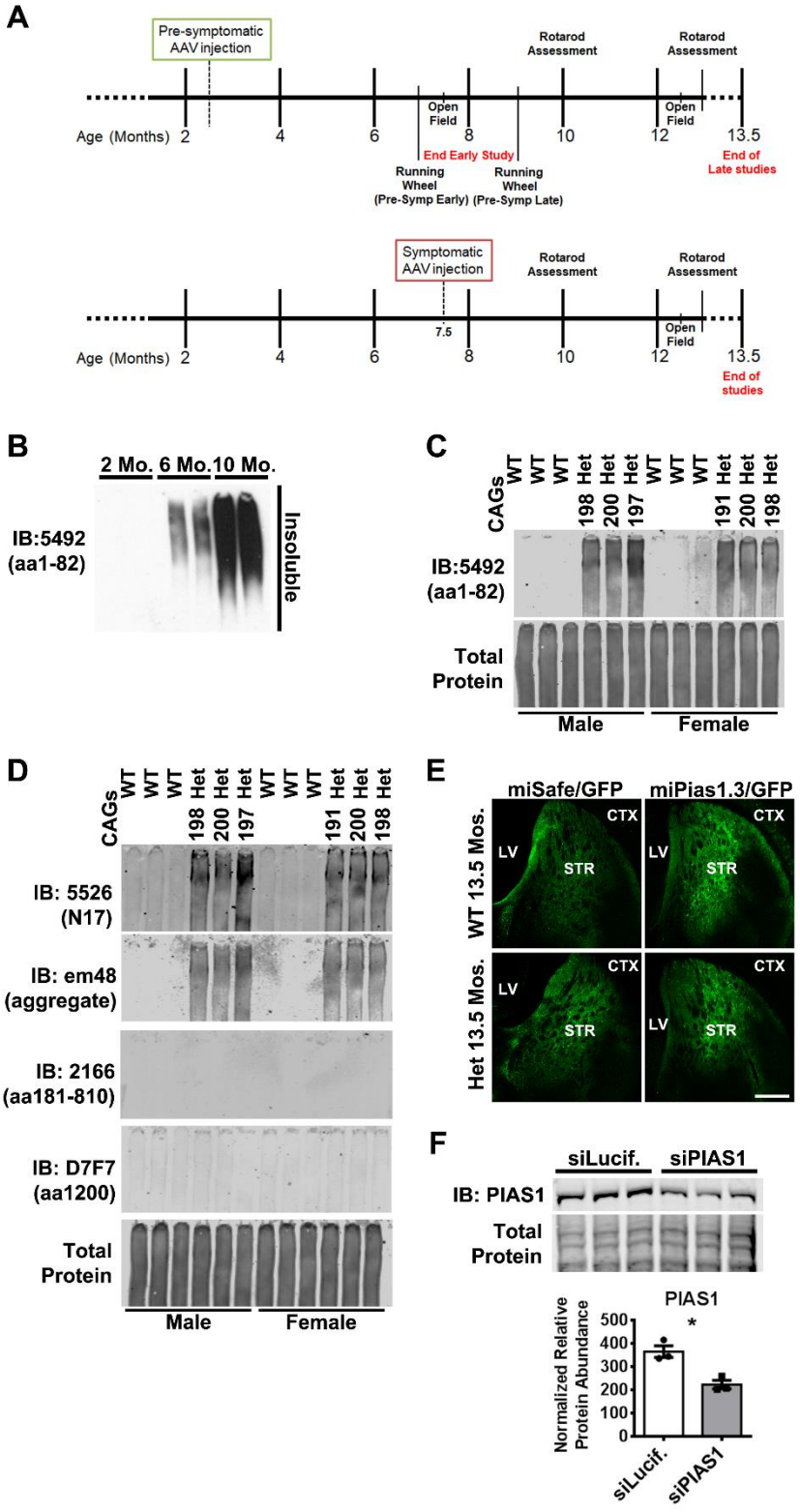

Supplemental Figure S1: **Efficiency of viral transduction and HWM mHTT formation in zQ175 mouse striatum.** A) Time-lines for presymptomatic and symptomatic injections of AAV2/1 miRNA, behavior, and sacrifice dates. B). Western blot indicating HMW Insoluble mHTT is detectable at 6 Mo, and increases at 10 Mo. C Insoluble HMW mHTT in both male and female zQ175 mice at 12 Mo is detectable by 5492 antibody, which was used for all subsequent assessments of this species and D) N-terminal recognizing antibodies only (n=3/sex). E) Mouse brain section showing GFP viral reporter is present 11 months post-injection, indicating continued presence of successful transduction (LV=Lateral Ventricle, STR=Striatum, CTX=Cortex) F) HeLa cell lysates with siRNA against PIAS1 and control siLuciferase shows specificity of Cell Signaling #3550 antibody against PIAS1 which was used for subsequent analysis (n=3). Protein normalized to total protein stain. HTT antibodies: 5526 (Abcam, ab109115), em38 (Millipore, MAB5374), 2166 (Millipore, MAB2166), D7F7 (Cell Signaling, 5656S), 5492 (Millipore MAB5492). Scale bar 500μm.

Supplemental Figure S2

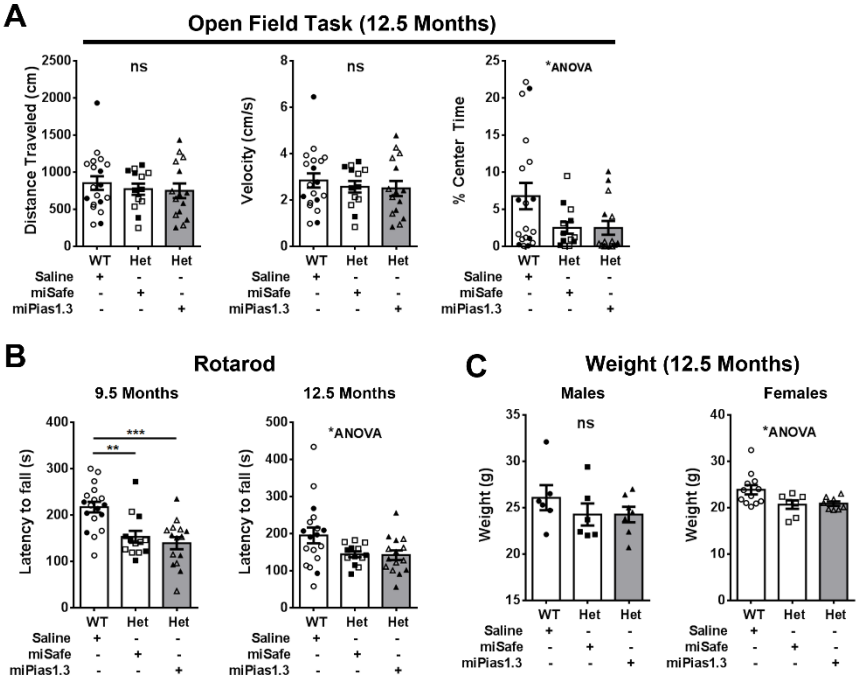

Supplemental Figure S2: Symptomatic Pias1 KD in zQ175 mice has no effect on behavior. A) Open field task at 12.5 Mo for combined group shows no effect for distance traveled or velocity but with a significant difference in % center time by 1-Way ANOVA, with no post-hoc reaching significance (males n=6-7, females n=7-13). B) Rotarod of combined males and females at 9.5 Mo (males n=6-7, females n=7-12) and 12.5 Mo (males n=6-7, females n=7-12) shows significant genotype effects but no treatment effects. C) No differences were detected in body weight at 12.5 Mo (males n=6-7, females n=7-12). Open symbols represent female mice. All samples were analyzed by 1-way ANOVA followed by Tukey's multiple comparison test. Statistical outputs are detailed in Supplemental Table 1. ns=not significant, *p<0.05, **p<0.01, ***p<0.001, values represent means ± SEM and individual values. Shaded bars represent miPias1.3 treated animals.

Supplemental Figure S3

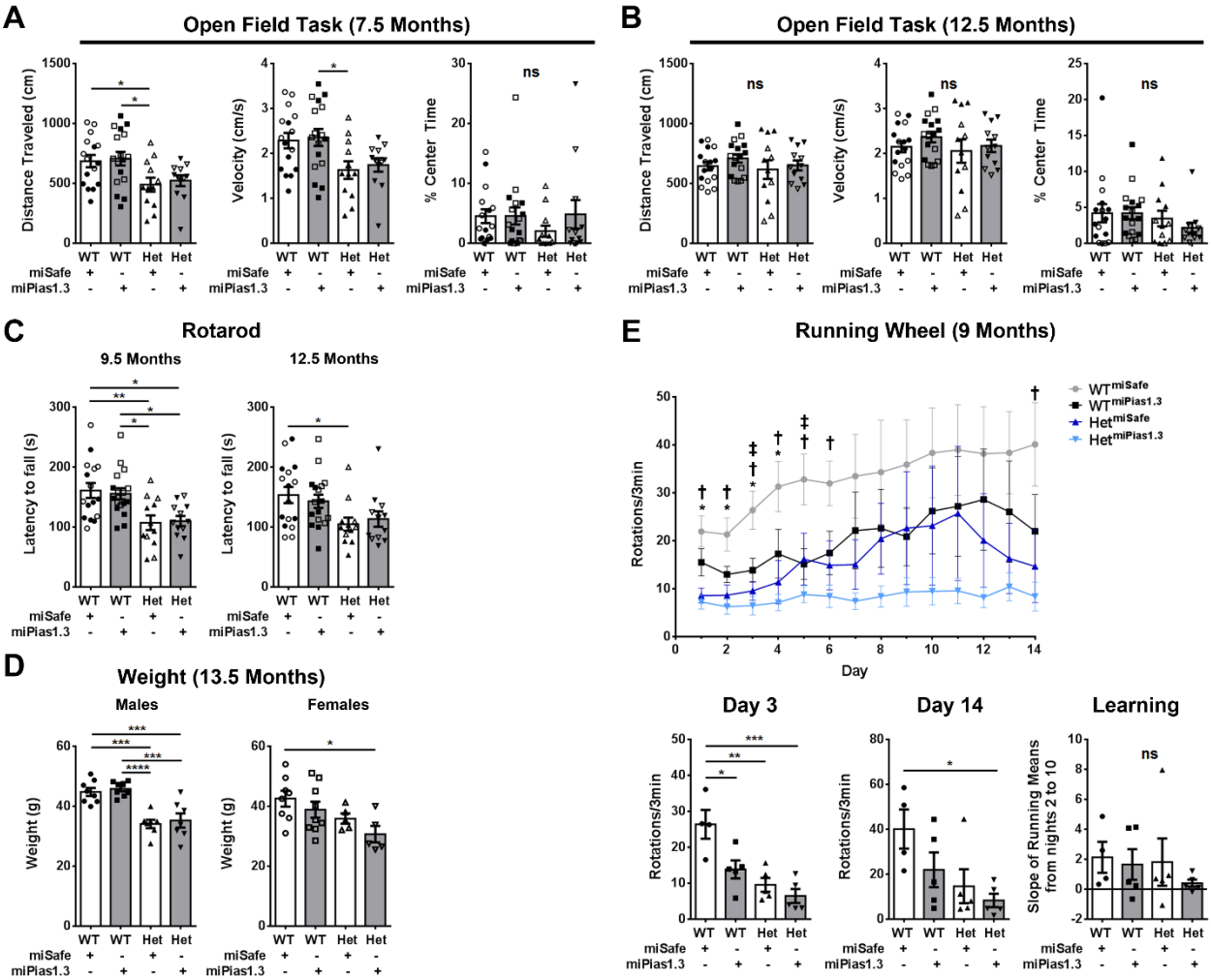

Supplemental Figure S3: **Presymptomatic Pias1 KD in zQ715 mice may exacerbate motor deficits.** A) Open field task at 7.5 Mo for combined group shows significant genotype effect for distance traveled and velocity but not % center time (males n=7-8, females n=5-9). B) No differences were detected in open field task at 12.5 Mo (males n=7-8, females n=5-9). C) Rotarod of combined males and females at 9.5 Mo (males n=7-8/group, females n=5-9/group) and 12.5 Mo (males n=7-8/group, females n=5-9/group) shows significant genotype effects. D) Male mice show genotype effect in body weight, only observed for females treated with miPias1.3 (males n=7-8/group, females n=5-9/group). E) Running wheel task at 9 Mo in males (n=4-5/group) suggests a negative impact on motor tasks with miPias1.3 treatment but with no effect on motor learning. Genotype effects were observed for day 1 ($F_{1, 15}$ = 21.620, p<0.001), day 2 ($F_{1, 15}$ = 19.320, p<0,001), day 3 ($F_{1, 15}$ = 22.230, p<0.001), day 4 ($F_{1, 15}$ = 12.230, p<0.01), day 5 ($F_{1, 15}$ = 7.879, p<0.05), day 6 ($F_{1, 15}$ = 9.265, p<0.001), day 7 ($F_{1, 15}$ = 6.986, p<0.05), day 12 ($F_{1, 15}$ = 4.887, p<0.05), day 13 ($F_{1, 15}$ = 5.751, p<0.05), and day 14 ($F_{1, 15}$ = 7.883, p<0.05). Treatment effects were observed for day 3 ($F_{1, 15}$ = 9.243, p<0.01) and Day 5 ($F_{1, 15}$ = 9.339, p<0.01). Overall variability may contribute to lack of observed differences. Open symbols represent female mice. All samples were analyzed by 2-way ANOVA followed by Tukey's multiple comparison test with additional statistical outputs detailed in Supplemental Table 1. ns=not significant, *p<0.05, **p<0.01, ***p<0.001, ****p<0.0001, values represent means ± SEM. Shaded bars represent miPias1.3 treated animals. For running wheel: ‡ = p<0.05 WT^{miSafe} vs $WT^{miPias1.3}$, * = p<0.05 WT^{miSafe} vs Het^{miSafe}, † = p<0.05 WT^{miSafe} vs $Het^{miPias1.3}$.

Supplemental Figure S4

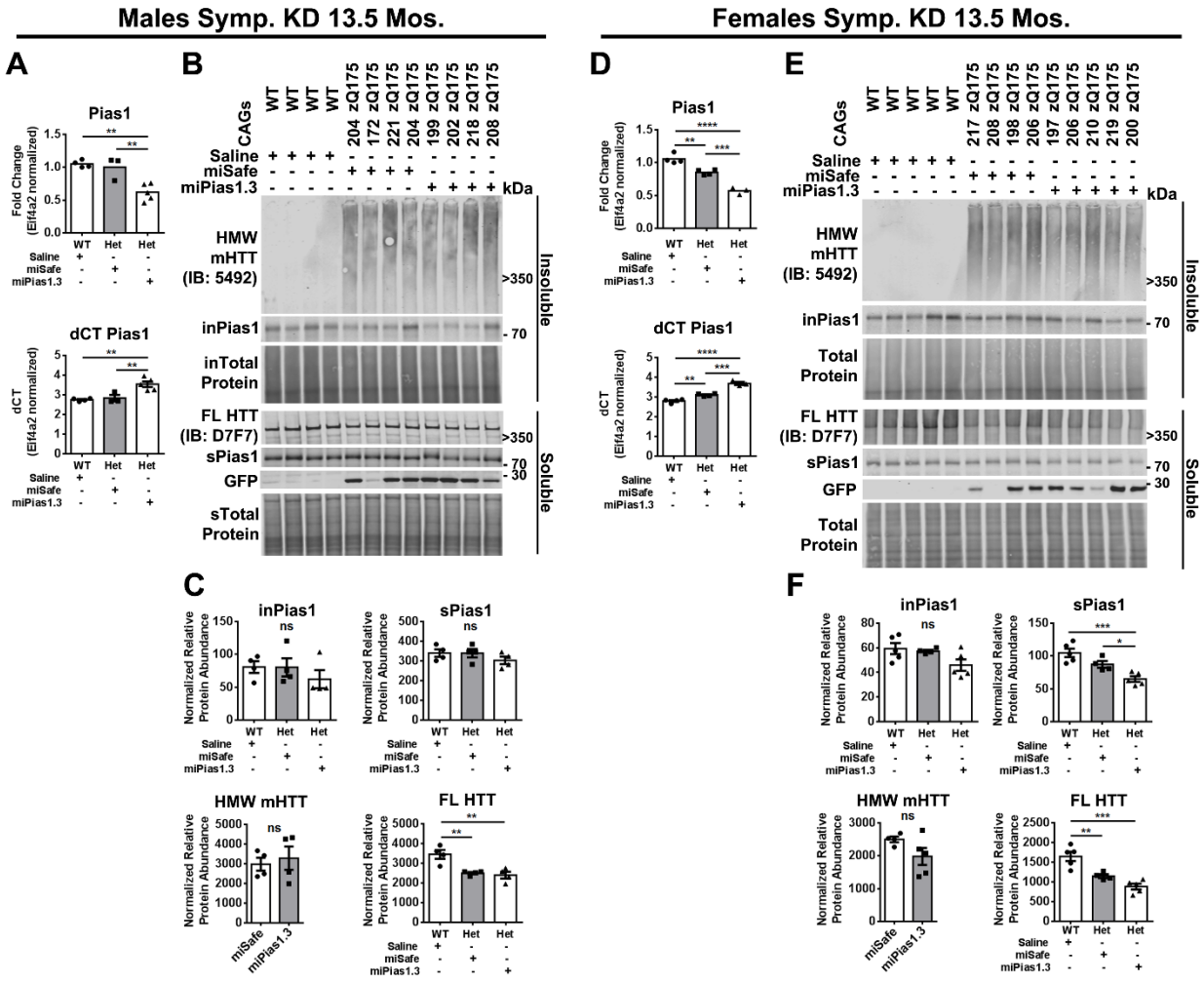

Supplemental Figure S4: **Symptomatic Pias1 KD does not affect mHTT accumulation at 13.5 months of age.** A) qPCR analysis of mRNA harvested from male GFP+ microdissected striata shows significant reduction in levels of Pias1 transcript with miPias1.3 treatment ($F_{2, 9}$ = 13.410, $p<0.01$). B) Western blot analysis of Soluble/Insoluble fractionation of striatal tissue from male mice and C) quantification shows no significant reduction of Pias1 protein in both fractions when detected with antibody validated against Pias1 (**SI Appendix, Figure S1F**). HMW insoluble mHTT detected with 5492 antibody remains unchanged with treatment. Soluble Full length (FL) HTT detected with D7F7 antibody shows a significant genotype effect with no treatment effect. D) qPCR analysis of mRNA harvested from female GFP+ microdissected striata shows significant reduction in levels of Pias1 transcript with miPias1.3 treatment as well as a significant genotype effect compared to WT vehicle control mice ($F_{2, 8}$ = 70.210, $p<0.0001$). E) Western blot analysis of Soluble/Insoluble fractionation of striatal tissue from female mice and F) quantification shows insufficient reduction of insoluble Pias1 protein but significant reduction of soluble Pias1 levels with miPias1.3 treatment. HMW insoluble mHTT remains unchanged with treatment. Soluble Full length (FL) HTT shows a significant genotype effect with no treatment effect. Protein normalized to total protein stain. Normalized relative protein abundances for all samples were analyzed by 1-way ANOVA followed by Tukey's multiple comparison test. ns = not significant, *$p<0.05$. **$p<0.01$, ***$p<0.001$, ****$p<0.0001$, values represent means ± SEM and individual values with n=3-5 animals analyzed per group. Shaded bars represent miPias1.3 treated animals.

Supplemental Figure S5

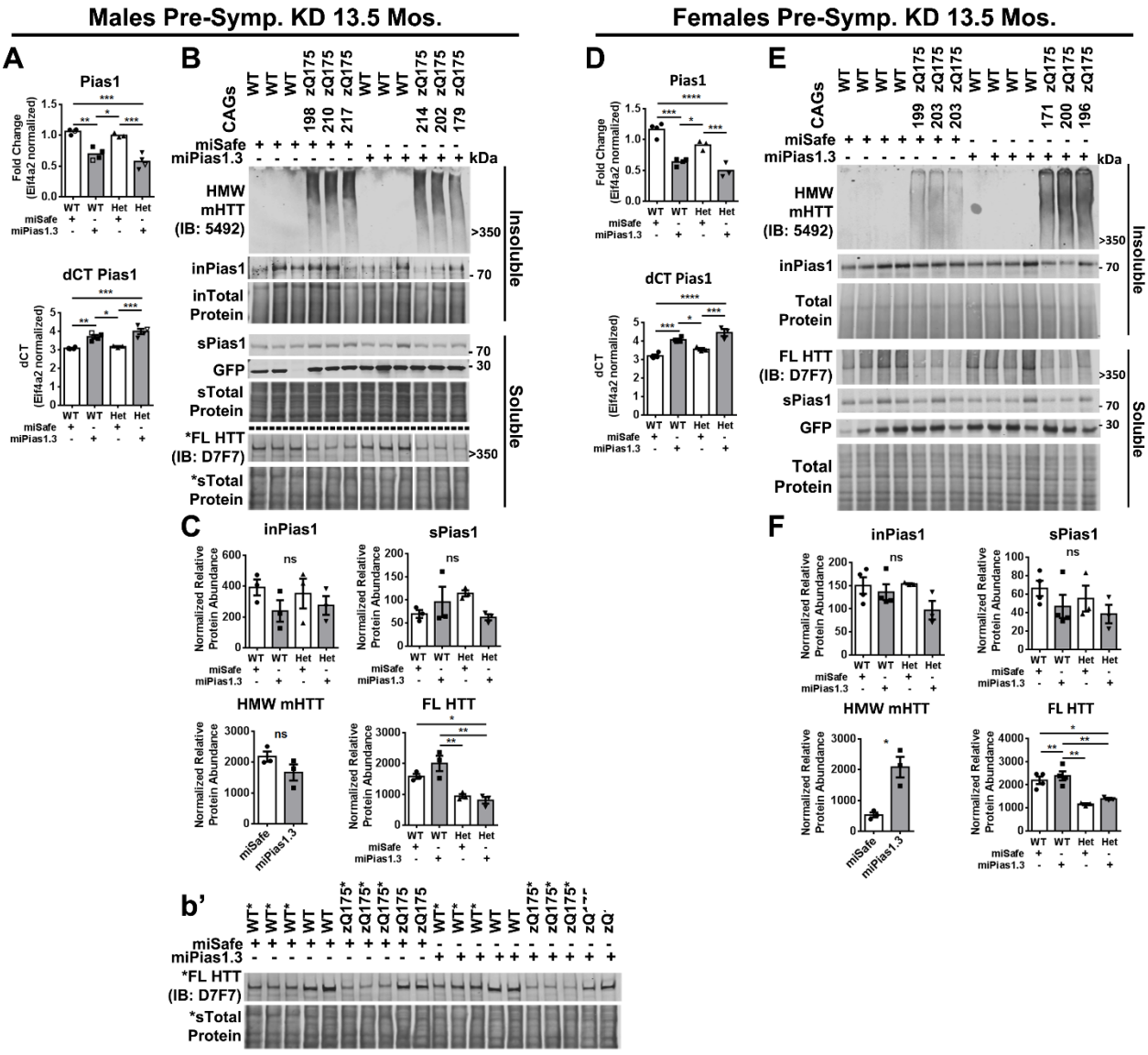

Supplemental Figure S5: **Presymptomatic Pias1 KD may affect mHTT accumulation at 13.5 months of age.** A) qPCR analysis of mRNA harvested from male GFP+ microdissected striata shows significant reduction in levels of Pias1 transcript with miPias1.3 treatment ($F_{1, 11} = 52.800$, $p<0.0001$). B) Western blot analysis of Soluble/Insoluble fractionation of striatal tissue from male mice and C) quantification shows no significant reduction of Pias1 protein in both fractions. HMW insoluble mHTT detected with 5492 antibody remains unchanged with treatment. Soluble Full length (FL) HTT detected with D7F7 antibody shows a significant genotype effect with no treatment effect. b') *samples used for representative image and quantitative analysis due to observed batch effect. *Samples all processed from the same batch. D) qPCR analysis of mRNA harvested from female GFP+ microdissected striata shows significant reduction in levels of Pias1 transcript with miPias1.3 treatment ($F_{1, 10} = 73.160$, $p<0.0001$). E) Western blot analysis of Soluble/Insoluble fractionation of striatal tissue from female mice and F) quantification shows no significant reduction of Pias1 protein in both fractions. HMW insoluble mHTT significantly increased with treatment. Soluble Full length (FL) HTT shows a significant genotype effect with no treatment effect. Solid symbols for qPCR represent samples used for later mRNAseq analysis. Protein normalized to total protein stain. Normalized relative protein abundances for all samples were analyzed by 2-way ANOVA followed by Tukey's multiple comparison test. ns = not significant, *$p<0.05$. **$p<0.01$, ***$p<0.001$, ****$p<0.0001$, values represent means ± SEM and individual values with n=3-4 animals analyzed per group. Shaded bars represent miPias1.3 treated animals.

Supplemental Figure S6

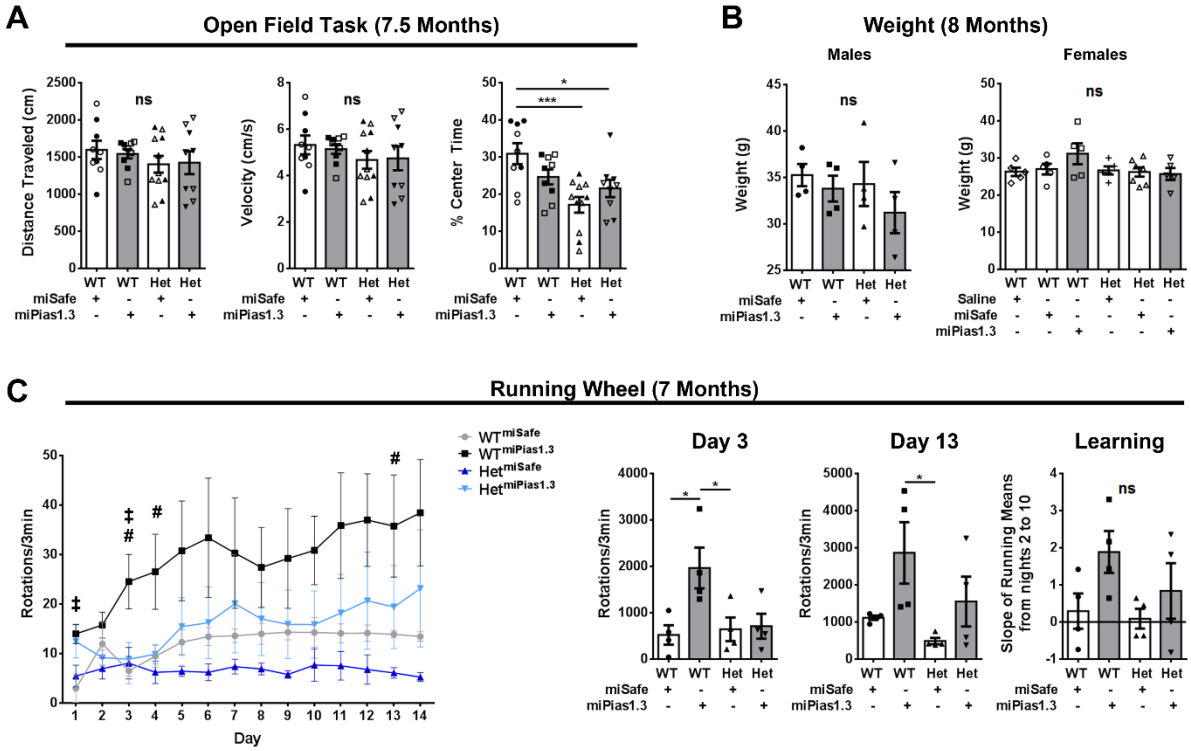

Supplemental Figure S6: **Presymptomatic Pias1 KD in zQ175 mice may rescue early motor deficits.** A) Open field task at 7.5 Mo for combined group shows no effect for distance traveled and velocity but a significant genotype effect for % center time (males n=4, females =5-7). B) No differences were detected in body weight at 8 Mo (males n=4, females =5-7). C) Running wheel task at 7 Mo in males suggests a significant increase in motor activity with miPias1.3 treatment in at least WT animals but with no effect on motor learning (n=4). Significant treatment effects were observed on day 1 ($F_{1, 12}$ = 11.840, p<0.01), day 3 ($F_{1, 12}$ = 6.053, p<0.05), day 4 ($F_{1, 12}$ = 6.019, p<0.05), day 5 ($F_{1, 12}$ = 5.292, p<0.05), day 10 ($F_{1, 12}$ = 5.390, p<0.05), day 11 ($F_{1, 12}$ = 5.646, p<0.05), day 12 ($F_{1, 12}$ = 6.882, p<0.05), day 13 ($F_{1, 12}$ = 6.921, p<0.05), and day 14 ($F_{1, 12}$ = 7.148, p<0.05). A significant interaction was detected on day 3 ($F_{1, 12}$ = 5.045, p<0.05). A significant genotype effect was detected on day 4 ($F_{1, 12}$ = 5.566, p<0.05). Open symbols represent female mice. All samples were analyzed by 2-way ANOVA followed by Tukey's multiple comparison test with additional statistical outputs detailed in Supplemental Table 1. ns=not significant, *p<0.05, ***p<0.001, values represent means ± SEM and individual values. Shaded bars represent miPias1.3 treated animals. For running wheel: ‡ = p<0.05 WT^{miSafe} vs $WT^{miPias1.3}$, # = p<0.05 $WT^{miPias1.3}$ vs Het^{miSafe}.

Supplemental Figure S7

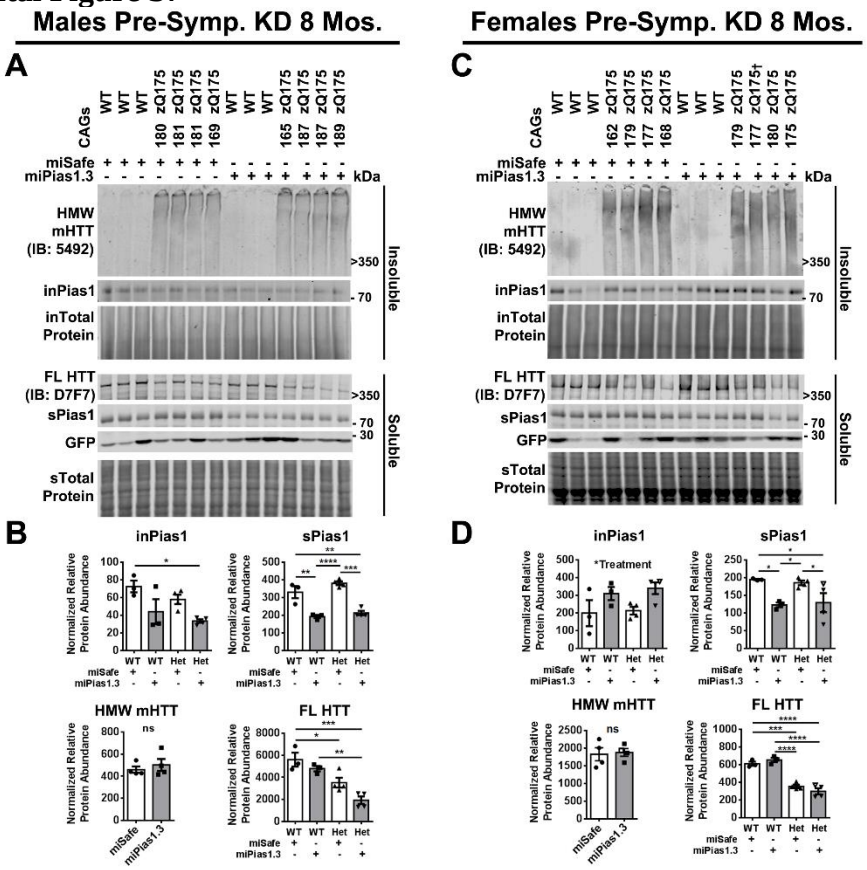

Supplemental Figure S7: **Soluble/Insoluble fractionation of 8-month-old presymptomatic treated zQ175 mice.** A) Western blots and B) quantification from male mice show significant reduction of Pias1 protein in both fractions. HMW insoluble mHTT detected by 5492 antibody remains unchanged with treatment at this age. Soluble Full length (FL) HTT detected by D7F7 antibody shows a significant genotype effect with a slight treatment effect observed with zQ175 animals having significantly less FL HTT than WT with miPias1.3 treatment. C) Western blots and D) quantification from Female mice show significant treatment effects for both Soluble and Insoluble but with wide variability. Soluble Pias1 levels in KD samples correspond to levels of GFP viral reporter. Excluding low-GFP expressing zQ175 sample (†, hollow graph symbol) reveals significant reduction of Pias1 in KD samples. FL HTT shows significant genotype effect only. Protein normalized to total protein stain, normalized relative protein abundances for all samples were analyzed by 2-way ANOVA followed by Tukey's multiple comparison test. ns = not significant, *p<0.05. **p<0.01, ***p<0.001, ****p<0.0001, values represent means ± SEM and individual values with n=3-4 animals analyzed per group. Shaded bars represent miPias1.3 treated animals.

Supplemental Figure S8

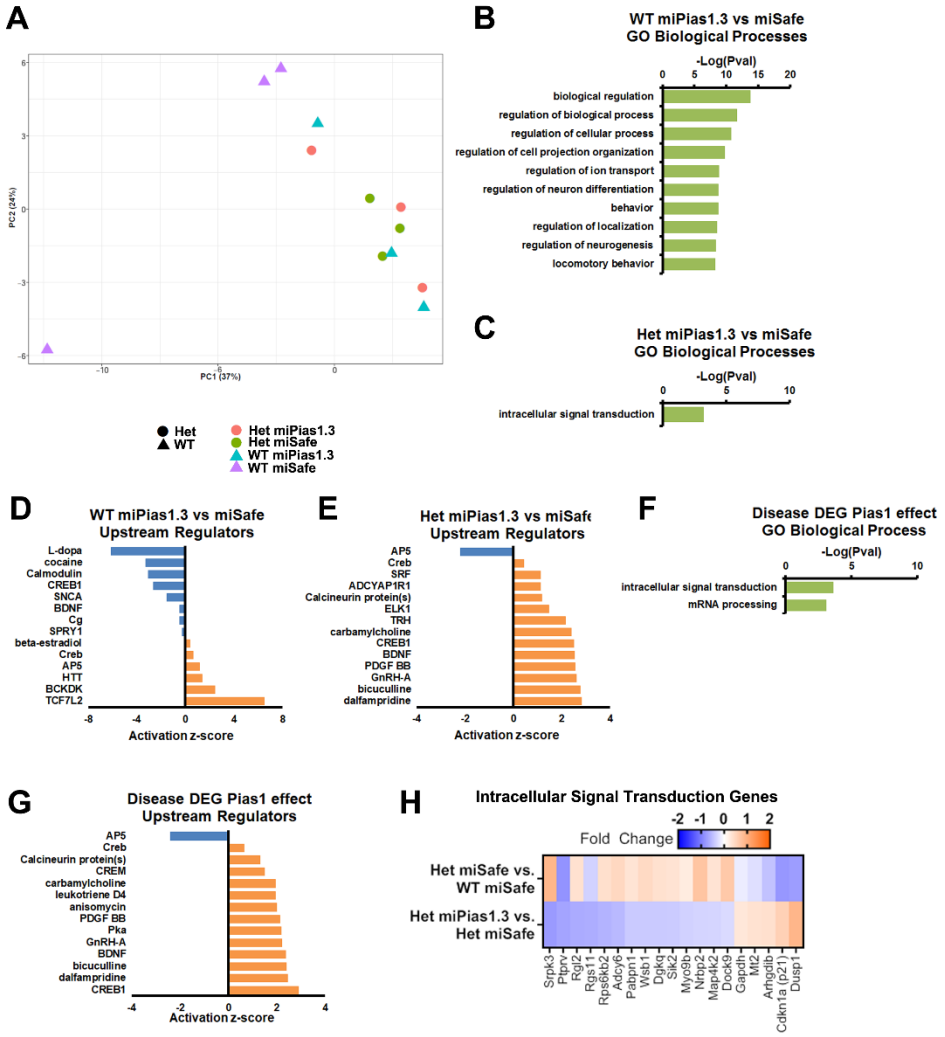

Supplemental Figure S8: Presymptomatic Pias1 KD has minimal effect on transcriptional landscape in males at 8 months of age. A) PCA of normalized gene expression values shows separation of WT treated animals. B) GO enrichment analysis of WT miPias1.3 vs miSafe treated animals and C) GO enrichment analysis of Het miPias1.3 vs miSafe treated animals. D) Top 10 IPA upstream regulators from WT miPias1.3 vs miSafe treated animals. E) Top 10 IPA upstream regulators from Het miPias1.3 vs miSafe treated animals. F) GO enrichment analysis of disease-associated DEGs (Disease DEG Pias1 effect). G) Disease-associated DEGs (Disease DEG Pias1 effect top 10 IPA upstream regulators. H) Fold change heatmap indicating normalizing effect of miPias1.3 treatment on disease-associated DEGs. n=3 animals per group.

Supplemental Figure S9

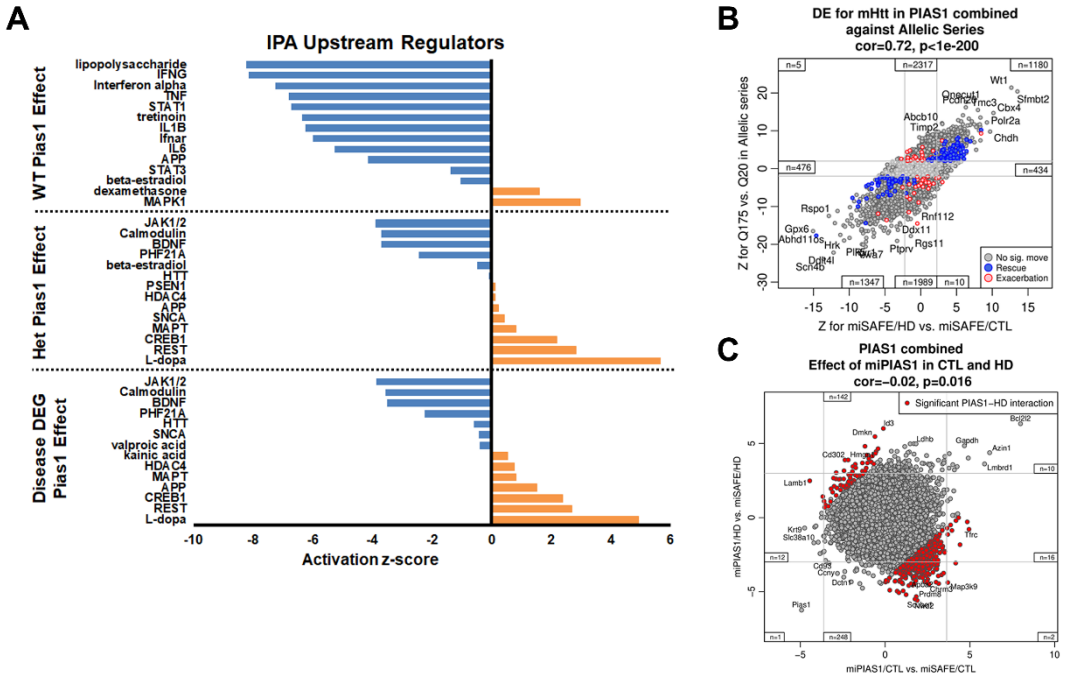

Supplemental Figure S9: Presymptomatic Pias1 KD modulates upstream regulators and has high concordance with previously published allelic series. At 13.5 mo. of age: A) Top 10 IPA terms for WT Pias1 effect (WT miPias1.3 vs. miSafe), Het Pias1 effect (Het miPias1.3 vs. miSafe), Overall Pias1 effect (279 genes shared between WT Pias1 effect and Het Pias1 effect), and Disease DEG Pias1 effect (521 disease-associated DEGs modulated by miPias1.3 treatment). B) Disease signatures from our zQ175 data shows highly significant positive correlation with published allelic series signatures (18). C) Significant anti-correlation is observed in genes changed between WT and Het miPias1.3 treated vs miSafe treated animals when compared to previously publishes allelic series data. n=3 animals per age per group.

Supplemental Figure S10

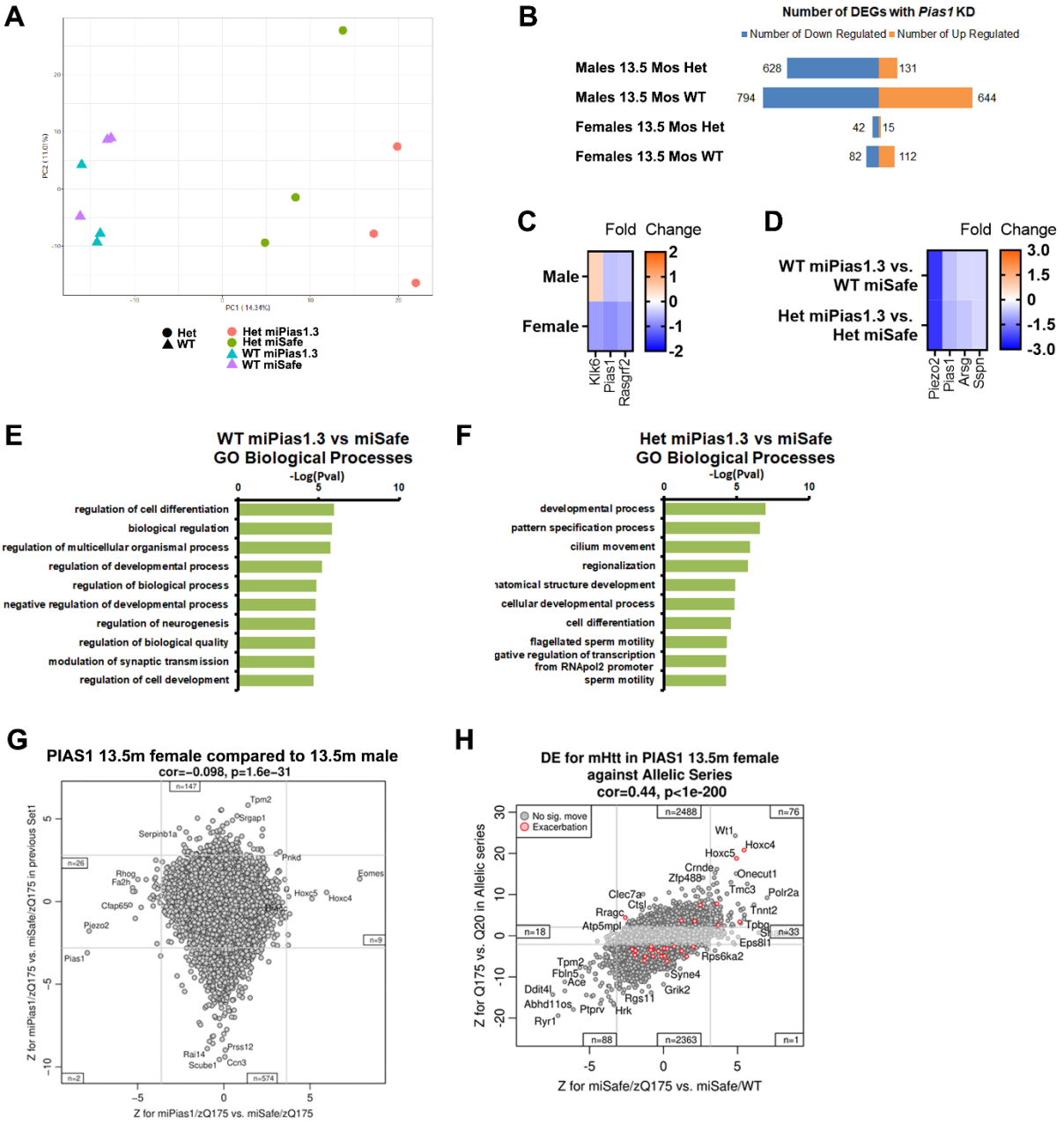

Supplemental Figure S10: **Presymptomatic Pias1 KD has minimal effect on transcriptional landscape in females.** A) PCA of normalized gene expression values shows separation by either genotype or treatment. B) Barplot showing number of DEGs per contrast between males and females at 13.5 mo. with Pias1 KD. C) Fold change heatmap of 3 shared DEGs between males and females at 13.5 mo. D) Fold change heatmap of treatment effect in both WT and Het females shows only 4 shared DEGs with Pias1 KD. E) GO enrichment analysis of WT miPias1.3 vs miSafe treated animals and GO enrichment analysis of Het miPias1.3 vs miSafe treated animals. G) Concordance analysis of Pias1 KD effect in females compared to males at 13.5 mo. suggests sex-dependent response. H) Female transcriptional signatures show a significant positive correlation with published allelic series signatures.

Supplemental Figure S11

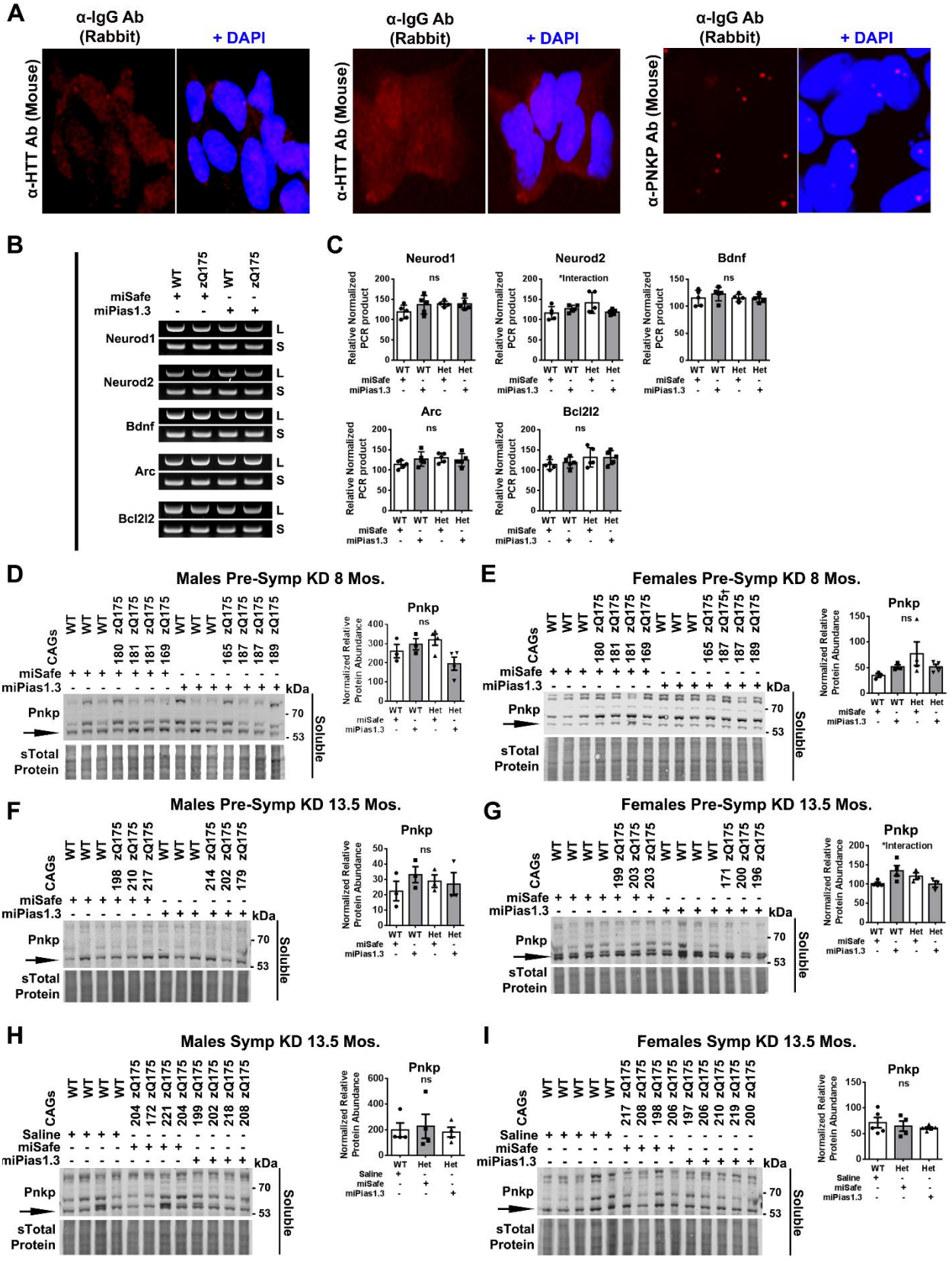

Supplemental Figure S11: Pias1 is part of the TCR complex but KD does not affect genomic stability in females or levels of Pnkp in vivo. A) Antigen controls for PLA in SH-SY5Y cells supports specific interaction between PNKP and HTT, HTT and PIAS1, and PNKP and PIAS1. B) LA-qPCR of normalized transcriptional targets in females (n=5/group) and C) quantification of PCR product. *Neurod1*: Treatment, $F_{1, 16} = 1.512$, $p>0.05$, Genotype, $F_{1, 16} = 2.319$, $p>0.05$, *Neurod2*: Treatment, $F_{1, 16} = 0.696$, $p>0.05$, Genotype, $F_{1, 16} = 1.346$, $p>0.05$, Interaction, $F_{1, 16} = 5.470$, $p<0.05$, *Bdnf*: Treatment, $F_{1, 16} = 0.529$, $p>0.05$, Genotype, $F_{1, 16} = 0.620$, $p>0.05$, *Arc*: Treatment, F1, 16 = 0.363, $p>0.05$, Genotype, F1, 16 = 1.179, $p>0.05$, *Bcl2l2*: Treatment, $F_{1, 16} = 0.073$, $p>0.05$, Genotype, $F_{1, 16} = 3.670$, $p<0.05$. Western blot analyses of D) presymptomatic miPias1.3 treatment in 8 Mo male mice does not affect levels of Pnkp protein (Genotype: $F_{1, 9} = 0.040$, $p>0.05$; Treatment: $F_{1, 9} = 0.970$, $p>0.05$). E) 8 Mo female mice with presymptomatic miPias1.3 treatment show no significant change in Pnkp levels both with (Genotype: $F_{1, 10} = 2.237$, $p>0.05$; Treatment: $F_{1, 10} = 0.102$, $p>0.05$) and without (Genotype: $F_{1, 9} = 2.081$, $p>0.05$; Treatment: $F_{1, 9} = 0.051$, $p>0.05$) low-GFP expressing zQ175 sample (†, hollow graph symbol). F) 13.5 Mo male mice with presymptomatic treatment show no differences in levels Pnkp (Genotype: $F_{1, 8} = 0.001$, $p>0.05$; Treatment: $F_{1, 8} = 0.552$, $p>0.05$). G) 13.5 Mo female mice with presymptomatic treatment show a significant interaction detected for levels of Pnkp but no significant post-hoc detected (Interaction: $F_{1, 9} = 8.001$, $p<0.05$). 13.5 Mo H) male and I) female mice with symptomatic treatment show no effect on levels of Pnkp protein (Males: $F_{2, 9} = 0.119$, $p>0.05$; Females: $F_{2, 11} = 0.490$, $p>0.05$). Black arrows indicated quantified Pnkp protein band detected by an antibody previously validated to detect endogenous Pnkp from mouse brain (34). Higher bands may represent post-translational modifications of Pnkp. Protein normalized to total protein stain. Panel A transferred onto 0.45 μm PVDF-FL, Panels B-F transferred onto 0.45 μm Nitrocellulose membranes. Normalized relative protein abundances for all samples for presymptomatic treated animals were analyzed by 2-way ANOVA followed by Tukey's multiple comparison test. All samples for symptomatic treated animals were analyzed by 1-way ANOVA followed by Tukey's multiple comparison test. Shaded bars represent miPias1.3 treated animals. Long amplicon (L) normalized to short amplicon (S). *$p<0.05$, , ns= not significant, values represent means ± SEM and individual values. n=3-5 animals analyzed per group.

Supplemental Figure S12

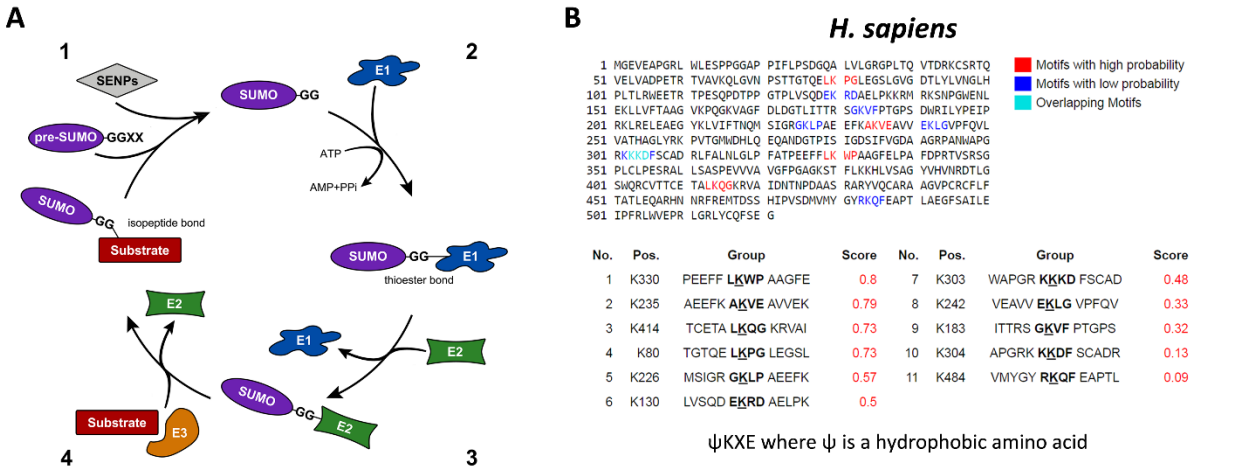

No.	Pos.	Group	Score	No.	Pos.	Group	Score
1	K330	PEEFF **LKWP** AAGFE	0.8	7	K303	WAPGR **KKKD** FSCAD	0.48
2	K235	AEEFK **AKVE** AVVEK	0.79	8	K242	VEAVV **EKLG** VPFQV	0.33
3	K414	TCETA **LKQG** KRVAI	0.73	9	K183	ITTRS **GKVF** PTGPS	0.32
4	K80	TGTQE **LKPG** LEGSL	0.73	10	K304	APGRK **KKDF** SCADR	0.13
5	K226	MSIGR **GKLP** AEEFK	0.57	11	K484	VMYGY **RKQF** EAPTL	0.09
6	K130	LVSQD **EKRD** AELPK	0.5				

Supplemental Figure S12: **PNKP may be a substrate for SUMOylation.** A) SUMO is covalently linked to target substrates through a four-step enzymatic pathway: 1) SUMO processing by SUMO-specific proteases (SENPs) expose the diglycine motif, 2) activation of SUMO by E1 activating enzymes generates a thioester bond, 3) SUMO transfer onto E2 conjugating enzyme followed by 4) transfer to E3 ligase through transthioesterification reactions to conjugate SUMO moiety onto target substrate. B) Human PNKP is predicted to be SUMOylated at numerous lysine residues by Abcepta SUMOplot™. C) Several predicted PNKP SUMO consensus sites are highly conserved in mammals and lower vertebrates. Human lysines are listed with corresponding alignments from Clustal Omega™ output. Yellow highlights conserved residues (compared to human) if consensus site was predicted by SUMOplot™.

Supplemental Figure S13

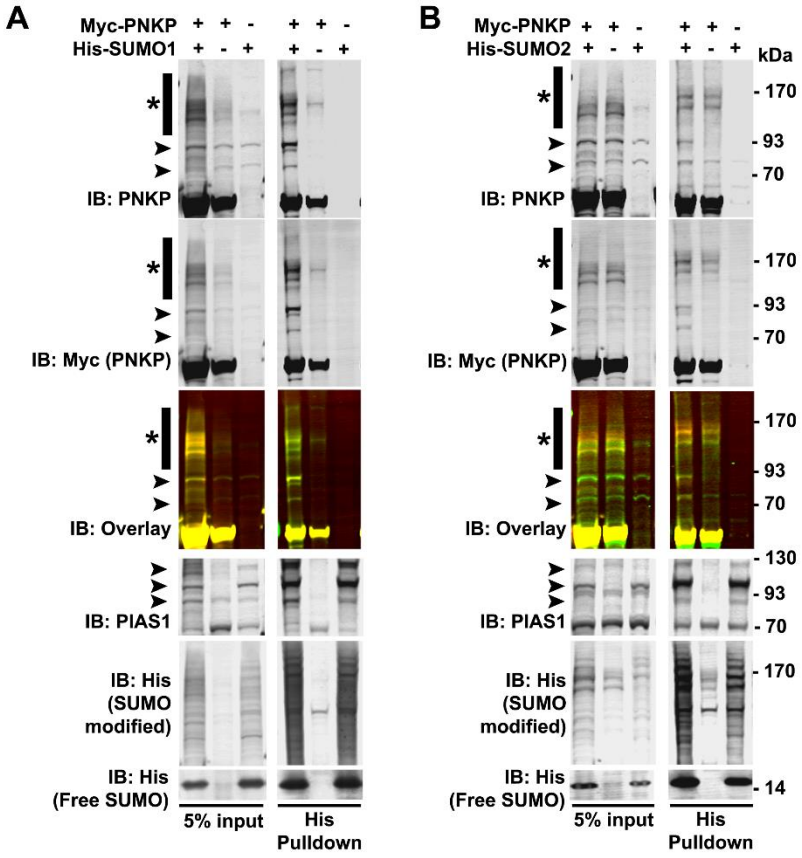

Supplemental Figure S13: PNKP is SUMOylated and may be a substrate for STUbL activity *in vitro*. PNKP is SUMOylated by A) SUMO1 and B) SUMO2 as shown using in-cell SUMOylation assay in HeLa cell-lysates assessed under denaturing conditions. Black arrowheads indicate corresponding molecular weight shift of SUMOylated substrate by numerous SUMO moieties. SUMOylated PIAS1 serves as a positive control. High molecular weight laddering after denaturing pulldown suggests PNKP is modified beyond two SUMO moieties. Asterisk indicated high molecular weight laddering. n=3 per SUMO isoform. Overlay (yellow) shows immunoreactivity of modified species with both anti-PNKP (green) and anti-Myc (red) antibodies.

Supplemental Figure S14

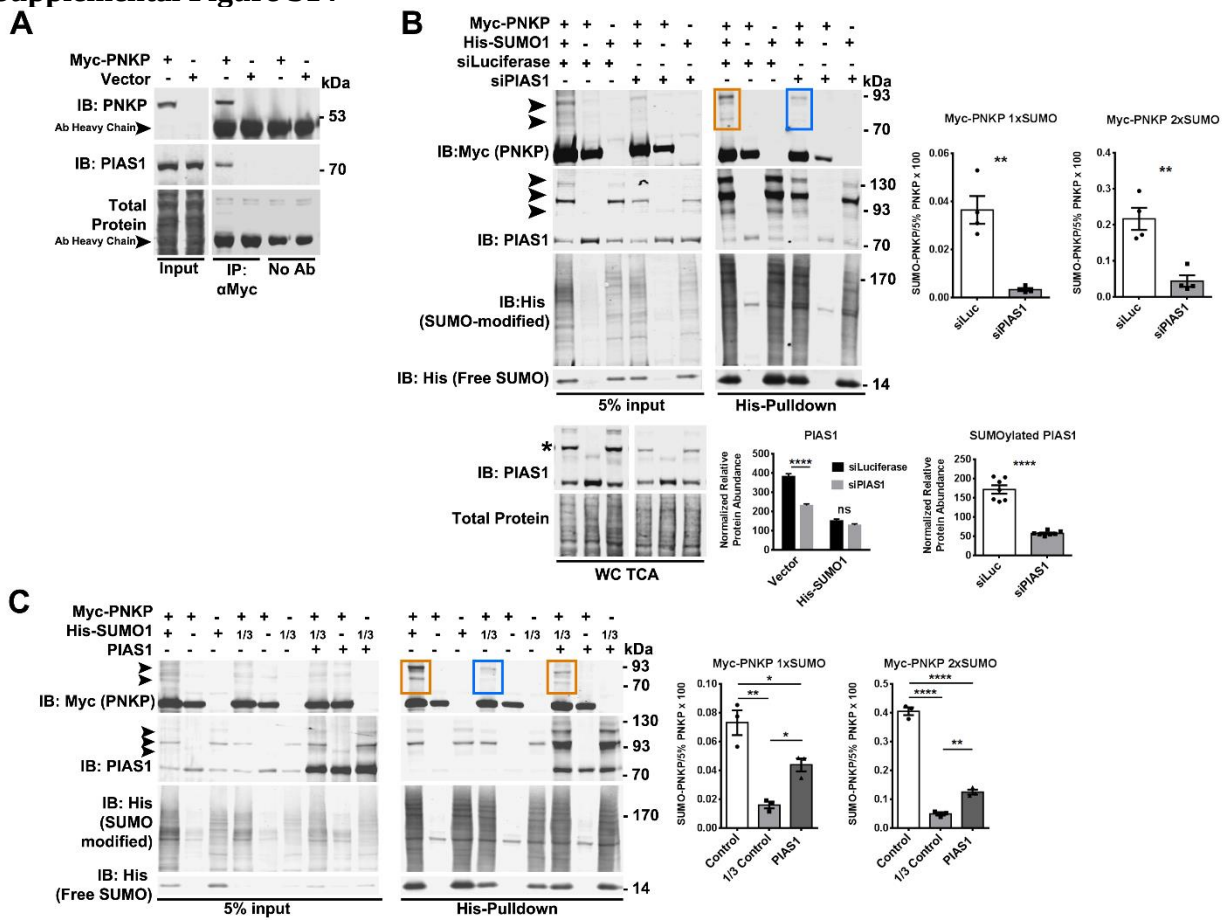

Supplemental Figure S14: SUMO1 PNKP modification is mediated by PIAS1 *in vitro*. A) HeLa cells transfected with myc-PNKP and subjected with Coimmunoprecipitation assay with anti-myc antibody shows specific interaction between myc-PNKP and endogenous PIAS1 in this cell type. Arrowheads represent antibody heavy chains. B) Significant knock-down ($p<0.0001$) of PIAS1 with siRNA (siPIAS1) shows a reduction in SUMOylated PNKP by His-SUMO1 ($p<0.01$, $n=4$). C) Under SUMO-limiting conditions (1/3 normal input), PIAS1 over expression significantly increases PNKP SUMOylation by His-SUMO1 (1xSUMO $F_{2,\ 6} = 24.34$, $p<0.01$, 2xSUMO $F_{2,\ 6} = 369.40$, $p<0.0001$, $n=3$). Asterisk represent SUMOylated PIAS1 used for quantification. *$p<0.01$, **$p<0.001$, ****$p<0.0001$, ns= not significant, values represent means ± SEM.

Supplemental Figure S15

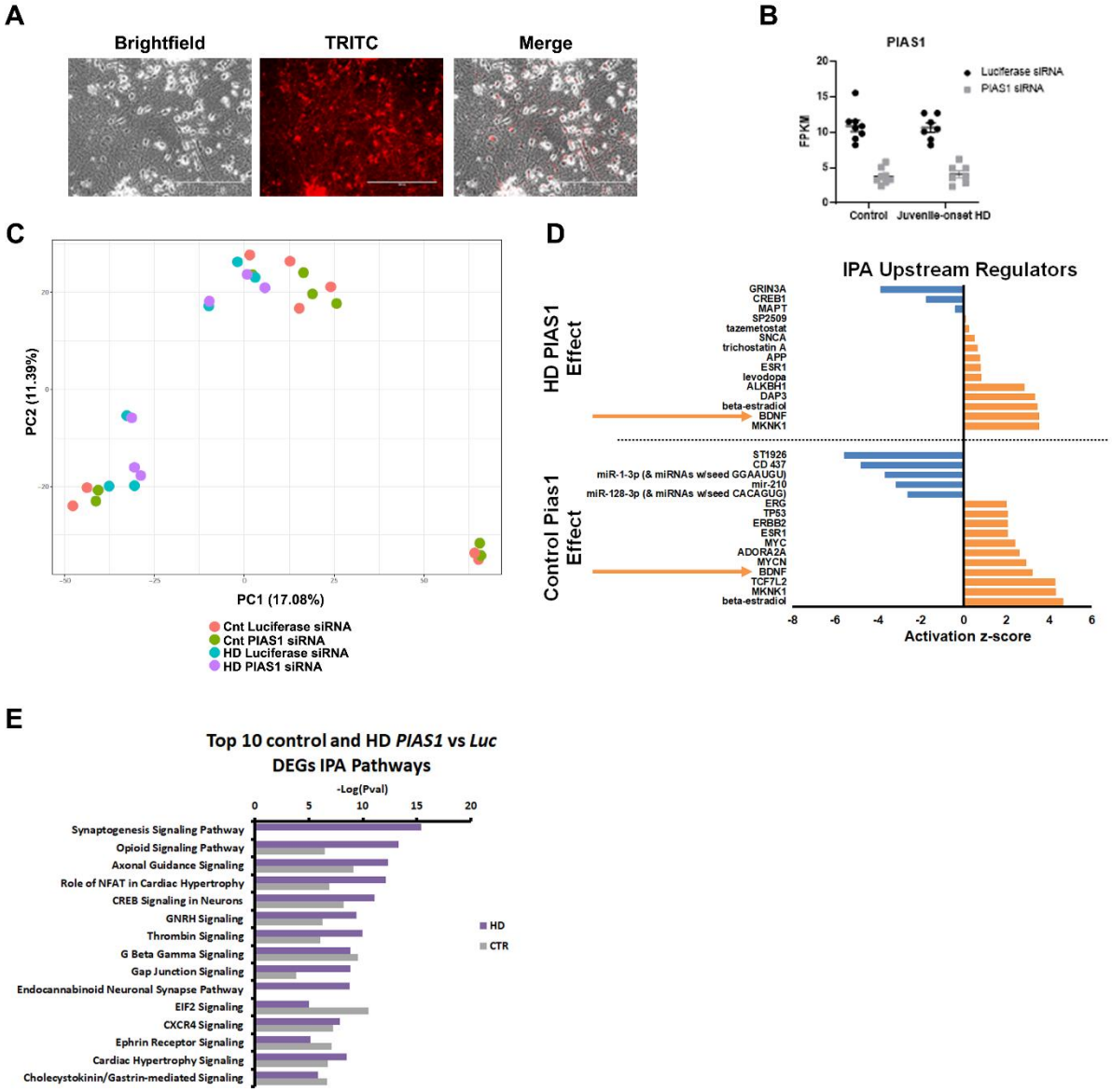

Supplemental Figure S15: Neuronal knockdown of PIAS1 in iPSC derived neurons mRNAseq. A) Representative images of LNP delivery efficiency from preliminary studies in the CS14iCTR28n6 iPSC line. LNPs were delivered on day 18 of differentiation as with remaining studies and the image taken 1 day later. LNPs contain a red fluorescent protein to mark delivery into cells. Scale bar = 200 µm B) FPKMs of PIAS1 in control (CS71iCTR20n6, CS83iCTR33n1, CS25iCTR18n6, CS14iCTR28n6), and HD (CS02iHD66n4, CS81iHD71n3, and CS09iHD109n4) samples showing all samples treated with PIAS1 siRNA had reduced expression of PIAS1 compared to control luciferase siRNA samples. C) PCA of normalized gene expression values shows most variance is cell line to cell line dependent. Key highlights cell line condition CTL vs HD and then siRNA treatment. D) Bar chart of the top 15 most significant IPA upstream regulator terms in order of activation score in control and HD samples assessing the PIAS1 effect blue bars show downregulated terms and orange show upregulated terms. Orange arrows highlight that BDNF is upregulated in both control and HD with PIAS1 knockdown. E) Top 10 IPA pathways from PIAS1 vs Luciferase siRNA control treated samples in control and HD cell lines.

Supplemental Figure S16

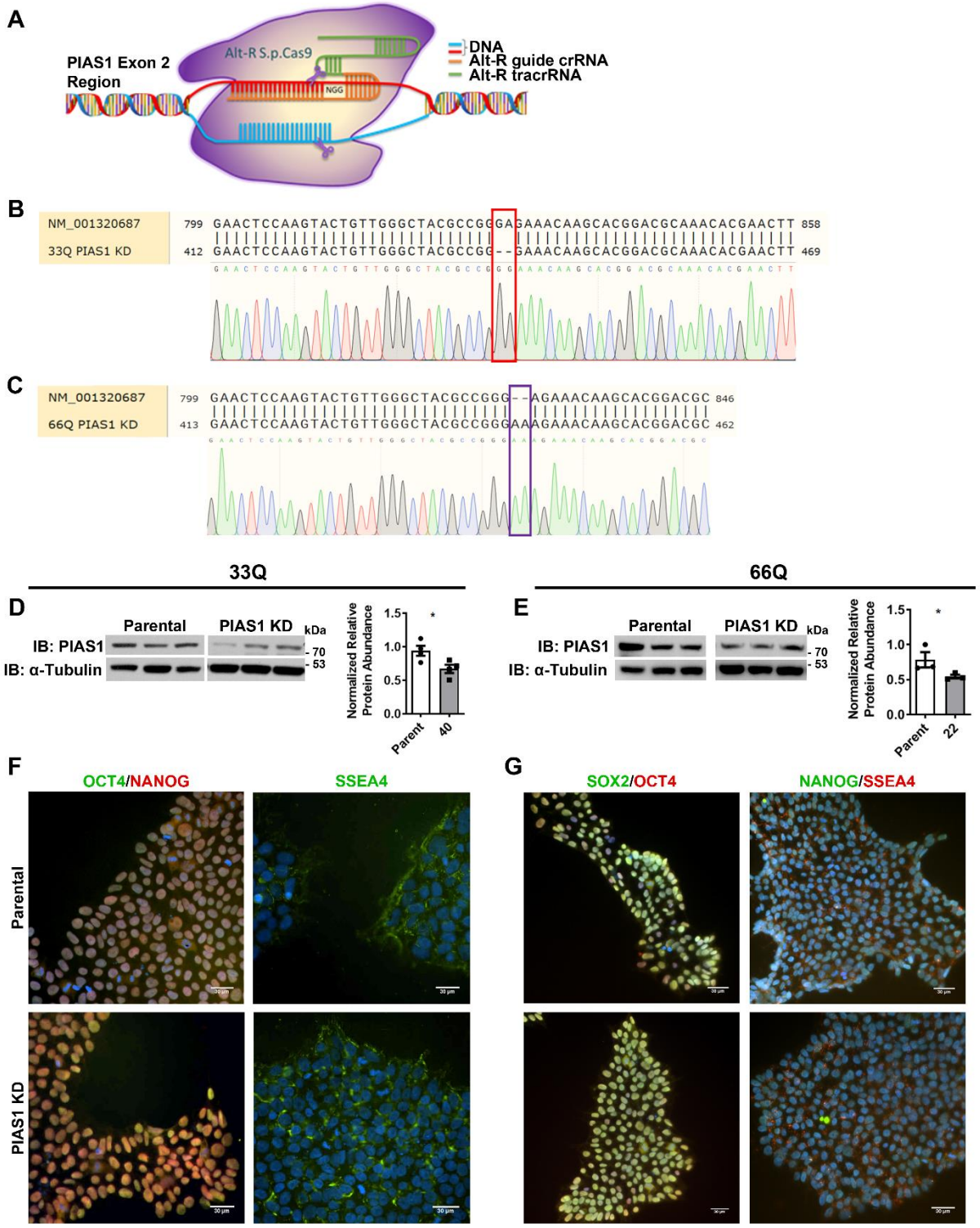

Supplemental Figure S16: Heterozygote CRISPR/Cas9 PIAS1 iPSCs show decreased PIAS1 protein levels without effecting pluripotency. A) Schematic showing CRISPR/Cas9 design to create an in-del mutation at the PIAS1 locus in exon 2. B) 33Q Clone 40 PIAS1 sequence highlighting the mutation a deletion in 33Q Clone 40 generating a *PIAS1* heterozygote line. C) 66Q Clone 22 *PIAS1* sequence highlighting the mutation an insertion in 66Q clone 22 generating a *PIAS1* heterozygote line. Western blots from D) 33Q and E) 66Q iPSCs lines modified at the PIAS1 locus by CRISPR/Cas9 generating PIAS1 heterozygotes showing significant decreases in PIAS1 protein levels ($p<0.05$, $n=3$). Quantification of the PIAS1 expression normalized to α-tubulin. Staining for pluripotency markers (NANOG, OCT4, SOX2 and SSEA4 in F) 33Q and G) 66Q gene edited clones shows no effect on pluripotency with levels the same between parental line and PIAS1 KD. * $p<0.05$, values represented as means ± SEM and individual values. Scalebar = 30 µm.

Supplemental Figure S17

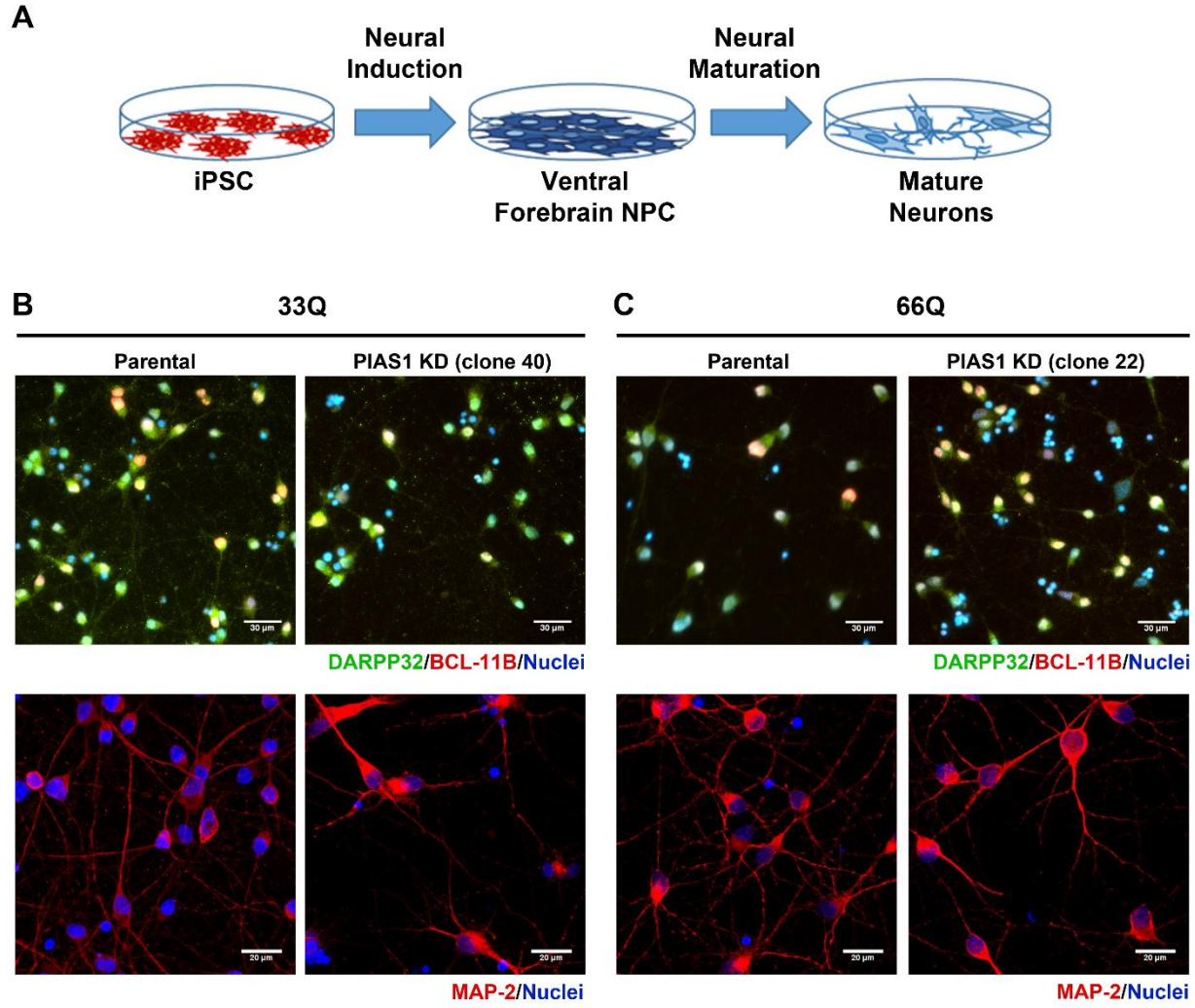

Supplemental Figure S17: Heterozygote CRISPR/Cas9 PIAS1 iPSCs can differentiate into neurons. A) Schematic of 37-day differentiation paradigm to make neurons enriched for medium spiny neurons of CRISPR edited PIAS1 knock-down clones and parental lines. Immunofluorescence of B) CRISPR modified iPSC 33Q parent and PIAS1 heterozygote and C) 66Q parent and PIAS1 heterozygote lines differentiated for 37 days to neurons for DARPP32 (green) BCL-11B (red) - top panel and MAP-2 (red) - bottom panel. Scalebar = 30 µm for top panels and 20 µm for bottom panels.

Supplementary Tables

Table S1

Gene Symbol	TPOTS	8mer	7mer-M8	7mer-1A	6mer
Aspg	0.231	1	1	0	1
Hsd17b11	0.225	1	0	1	0
Synj2bp	0.21	0	3	0	0
Cd44	0.161	1	0	0	1
Zkscan1	0.16	1	0	0	0
Zfp819	0.16	1	0	0	0
Tirap	0.16	1	0	0	0
Tbc1d16	0.16	1	0	0	0
Sik1	0.16	1	0	0	0
Rfwd3	0.16	1	0	0	0
Pdgfb	0.16	1	0	0	0
Il16	0.16	1	0	0	0
Hp1bp3	0.16	1	0	0	0
Gpx5	0.16	1	0	0	0
Ffar2	0.16	1	0	0	0
Elovl6	0.16	1	0	0	0
Dlx1	0.16	1	0	0	0
Dlk1	0.16	1	0	0	0
Dgcr8	0.16	1	0	0	0
Ces2g	0.16	1	0	0	0
Celf4	0.16	1	0	0	0
Cbx4	0.16	1	0	0	0
Adipor2	0.16	1	0	0	0
Abhd4	0.16	1	0	0	0
3830431G21Rik	0.16	1	0	0	0
2310003L22Rik	0.16	1	0	0	0
1700058C13Rik	0.16	1	0	0	0
Sap18	0.141	0	2	0	1
Rc3h2	0.135	0	1	1	0
Pde4a	0.135	0	1	1	0

Table S1: List of potential off-target genes for miPias1.3 determined by siSPOTR

Table S2

Species	Gene Target	Forward (5'->3')	Reverse (5'->3')
Mouse	*Eif4a2*	GTGGACTGGCTCACGGAGAAAA	AGAACACGGCTTGACCCTGATC
Mouse	*Pias1*	CTGCACAGACTGTGACGAGATAC	CGCTACCTGATGCTCCAATGTG

Table S2: List of mouse primers used for qPCR

Table S3

		Long Amplicon		Short Amplicon	
Species	**Gene Target**	**Forward (5'->3')**	**Reverse (5'->3')**	**Forward (5'->3')**	**Reverse (5'->3')**
Mouse	NeuroD1	ATCAAGCACC ACATAGGCAA ACCACA	GCTCAGCATC AGCAACTCGG CTA	GGGAGAGAG GCAAGCAGAA GAAGAA	TAGGAAAGGC ACCCATAGCC ACTCA
Mouse	NeuroD2	GCTCATCTTA CCATCTCACC AGGGC	GCATGCCAAT CACCGTCTCT CATGT	CTCCTCCACG AAGAGACACT GGCTT	CCCTCACTCT GTGCTGTCTG TCTCC
Mouse	Bdnf	ACCACTGTGC TGCATTCTTA GCACT	ACCCAAGACC ACTGCCATAC AACTG	CCAGTTTTCTC CATGTGCTCA GGCT	TCTTTGTTGCT CACCTTTACG ACACC
Mouse	Arc	TGACAGGCTT CAGCAAGACA GAAGG	ACATTAGTCA CTCGGGGCTG TGAAG	GAGAACTCGC TTGAGCTCTG CACC	ATTAGTCACT CGGGGCTGTG AAGG
Mouse	Bcl2l2	ATTCAGCCCC TGTCTCCTCC CTATC	ACCAGGCTGC TTCATTTCAG CTTTG	GTGGCATTCT TTGTCTTTGG GGCTG	CTTTGTAGAG GGATGCGGAG AGCAG
Human	NEUROD1	CCTTGACTGA CTGAAAGAAT CCCTA	GCATACAAAT GGGCAGGTCA C	AGGGAGAGGC AAACAGAAAG AAAAGCA	ACACGCACGC GCCATTATAA AACAC
Human	BDNF	TGTGAGGGAG GTCTACTTGG CAGAA	CCTTTCCCCC ATCCTTGTGTT TCCA	TGAGATGTCA GAACATTTTC CCGTG	AGGCTTTGAA GGGATTCTGT TGGGT
Human	BCL2L2	GTTGCCTCTTT CTGGCCTTTG GTTG	AATGTCCTGA CCCCAGGCTA TACAGT	CATCCTTCTG CAAAGCTGGT CTCCA	AAAGTCCCTG ACAACATTCC CCTGC
Human	mtDNA	TTTCATCATG CGGAGATGTT GGATGG	TCTAAGCCTC CTTATTCGAG CCGA	CCCCACAAAC CCCATTACTA AACCCA	TTTCATCATG CGGAGATGTT GGATGG

Table S3: List of primers used for LA-qPCR for both mouse and human genes.

Legends for Datasets S1-S7

Dataset S1: Detailed statistical outputs for animal behavioral data in both presymptomatic and symptomatic miPias1.3 treated animal cohorts. See excel sheet Supplemental Dataset S1 and corresponding tabs.

Dataset S2: List of genes analyzed for statistically significant differences from RNAseq from presymptomatic miPias1.3 treated males at both 8 and 13.5 Mo. and females at 13.5 Mo. See excel sheet Supplemental Dataset S2 and corresponding tabs for different ages and treatment comparisons.

Dataset S3: List of enriched GO processes from RNAseq from presymptomatic miPias1.3 treated males at both 8 and 13.5 mo. See excel sheet Supplemental Dataset S3 and corresponding tabs for different ages and treatment comparisons.

Dataset S4: List of enriched IPA Upstream Regulators analysis from RNAseq from presymptomatic miPias1.3 treated males at both 8 and 13.5 mo. See excel sheet Supplemental Dataset S4 and corresponding tabs for different ages and treatment comparisons.

Dataset S5: List of statistically significant genes, GO processes, and IPA Upstream Regulators from RNAseq from presymptomatic miPias1.3 treated males at both 8 and 13.5 Mo that were normalized by miPias1.3 treatment in zQ175 mice compared to disease-specific dysregulated genes. See excel sheet Supplemental Dataset S5 and corresponding tabs for different ages and treatment comparisons.

Dataset S6: List of HD-associated transcriptional co-expression modules and effect of miPias1.3 knock-down for rescue analysis. See excel sheet Supplemental Dataset S6.

Dataset S7: List of genes identified in iPSC-neuron RNAseq for the four different comparisons: PIAS1 siRNA treatment vs. Luciferase siRNA treatment in control neurons: Columns A-G, PIAS1 siRNA treatment vs. Luciferase siRNA treatment in HD neurons: Columns H-N, HD neurons vs. Control neurons treated with Luciferase siRNA: Columns O-U and HD neurons vs. Control neurons in PIAS1siRNA treated samples: Columns V-AB. See excel sheet Supplemental Dataset S7.

Supplemental References

1. L. B. Menalled *et al.*, Comprehensive behavioral and molecular characterization of a new knock-in mouse model of Huntington's disease: zQ175. *PloS one* **7**, e49838 (2012).
2. M. A. Hickey *et al.*, Extensive early motor and non-motor behavioral deficits are followed by striatal neuronal loss in knock-in Huntington's disease mice. *Neuroscience* **157**, 280-295 (2008).
3. J. Ochaba, E. L. Morozko, J. G. O'Rourke, L. M. Thompson, Fractionation for Resolution of Soluble and Insoluble Huntingtin Species. *Journal of visualized experiments : JoVE* 10.3791/57082 (2018).
4. J. Ochaba *et al.*, PIAS1 Regulates Mutant Huntingtin Accumulation and Huntington's Disease-Associated Phenotypes In Vivo. *Neuron* **90**, 507-520 (2016).
5. N. R. Franich *et al.*, Striatal Mutant Huntingtin Protein Levels Decline with Age in Homozygous Huntington's Disease Knock-In Mouse Models. *Journal of Huntington's disease* **7**, 137-150 (2018).
6. M. I. Love, W. Huber, S. Anders, Moderated estimation of fold change and dispersion for RNA-seq data with DESeq2. *Genome biology* **15**, 550 (2014).
7. C. Smith-Geater *et al.*, Aberrant Development Corrected in Adult-Onset Huntington's Disease iPSC-Derived Neuronal Cultures via WNT Signaling Modulation. *Stem cell reports* **14**, 406-419 (2020).
8. T. Heikkinen *et al.*, Characterization of neurophysiological and behavioral changes, MRI brain volumetry and 1H MRS in zQ175 knock-in mouse model of Huntington's disease. *PloS one* **7**, e50717 (2012).
9. A. L. Southwell *et al.*, An enhanced Q175 knock-in mouse model of Huntington disease with higher mutant huntingtin levels and accelerated disease phenotypes. *Human molecular genetics* **25**, 3654-3675 (2016).
10. E. A. Spronck *et al.*, AAV5-miHTT Gene Therapy Demonstrates Sustained Huntingtin Lowering and Functional Improvement in Huntington Disease Mouse Models. *Molecular therapy. Methods & clinical development* **13**, 334-343 (2019).
11. B. Zeitler *et al.*, Allele-selective transcriptional repression of mutant HTT for the treatment of Huntington's disease. *Nature medicine* **25**, 1131-1142 (2019).
12. S. Chamniansawat, S. Chongthammakun, Estrogen stimulates activity-regulated cytoskeleton associated protein (Arc) expression via the MAPK- and PI-3K-dependent pathways in SH-SY5Y cells. *Neuroscience letters* **452**, 130-135 (2009).
13. M. Blurton-Jones, P. N. Kuan, M. H. Tuszynski, Anatomical evidence for transsynaptic influences of estrogen on brain-derived neurotrophic factor expression. *The Journal of comparative neurology* **468**, 347-360 (2004).
14. M. Yao, T. V. Nguyen, C. J. Pike, Estrogen regulates Bcl-w and Bim expression: role in protection against beta-amyloid peptide-induced neuronal death. *The Journal of neuroscience : the official journal of the Society for Neuroscience* **27**, 1422-1433 (2007).
15. F. Sohrabji, R. C. Miranda, C. D. Toran-Allerand, Identification of a putative estrogen response element in the gene encoding brain-derived neurotrophic factor. *Proceedings of the National Academy of Sciences of the United States of America* **92**, 11110-11114 (1995).
16. B. Gegenhuber, J. Tollkuhn, Signatures of sex: Sex differences in gene expression in the vertebrate brain. *Wiley interdisciplinary reviews. Developmental biology* **9**, e348 (2020).

17. M. Gershoni, S. Pietrokovski, The landscape of sex-differential transcriptome and its consequent selection in human adults. *BMC biology* **15**, 7 (2017).
18. P. Langfelder *et al.*, Integrated genomics and proteomics define huntingtin CAG length-dependent networks in mice. *Nature neuroscience* **19**, 623-633 (2016).
19. H. i. Consortium, Developmental alterations in Huntington's disease neural cells and pharmacological rescue in cells and mice. *Nature neuroscience* **20**, 648-660 (2017).
20. J. G. O'Rourke *et al.*, SUMO-2 and PIAS1 modulate insoluble mutant huntingtin protein accumulation. *Cell reports* **4**, 362-375 (2013).
21. A. J. Kedaigle *et al.*, Treatment with JQ1, a BET bromodomain inhibitor, is selectively detrimental to R6/2 Huntington's disease mice. *Human molecular genetics* **29**, 202-215 (2020).
22. R. L. Boudreau, R. M. Spengler, B. L. Davidson, Rational design of therapeutic siRNAs: minimizing off-targeting potential to improve the safety of RNAi therapy for Huntington's disease. *Molecular therapy : the journal of the American Society of Gene Therapy* **19**, 2169-2177 (2011).
23. R. L. Boudreau *et al.*, siSPOTR: a tool for designing highly specific and potent siRNAs for human and mouse. *Nucleic acids research* **41**, e9 (2013).
24. P. Langfelder, S. Horvath, Fast R Functions for Robust Correlations and Hierarchical Clustering. *Journal of statistical software* **46** (2012).
25. C. Y. D. Lee *et al.*, Elevated TREM2 Gene Dosage Reprograms Microglia Responsivity and Ameliorates Pathological Phenotypes in Alzheimer's Disease Models. *Neuron* **97**, 1032-1048 e1035 (2018).
26. A. Chatterjee *et al.*, The role of the mammalian DNA end-processing enzyme polynucleotide kinase 3'-phosphatase in spinocerebellar ataxia type 3 pathogenesis. *PLoS genetics* **11**, e1004749 (2015).
27. R. Gao *et al.*, Mutant huntingtin impairs PNKP and ATXN3, disrupting DNA repair and transcription. *eLife* **8** (2019).
28. S. M. Mandal *et al.*, Role of human DNA glycosylase Nei-like 2 (NEIL2) and single strand break repair protein polynucleotide kinase 3'-phosphatase in maintenance of mitochondrial genome. *The Journal of biological chemistry* **287**, 2819-2829 (2012).
29. L. Wiederhold *et al.*, AP endonuclease-independent DNA base excision repair in human cells. *Molecular cell* **15**, 209-220 (2004).
30. A. Chakraborty *et al.*, Classical non-homologous end-joining pathway utilizes nascent RNA for error-free double-strand break repair of transcribed genes. *Nature communications* **7**, 13049 (2016).
31. J. H. Santos, J. N. Meyer, B. S. Mandavilli, B. Van Houten, Quantitative PCR-based measurement of nuclear and mitochondrial DNA damage and repair in mammalian cells. *Methods Mol Biol* **314**, 183-199 (2006).
32. J. A. Kulkarni et al., On the Formation and Morphology of Lipid Nanoparticles Containing Ionizable Cationic Lipids and siRNA. ACS nano 12, 4787-4795 (2018).
33. J. A. Kulkarni et al., Rapid synthesis of lipid nanoparticles containing hydrophobic inorganic nanoparticles. Nanoscale 9, 13600-13609 (2017).
34. M. Shimada, L. C. Dumitrache, H. R. Russell, P. J. McKinnon, Polynucleotide kinase-phosphatase enables neurogenesis via multiple DNA repair pathways to maintain genome stability. *The EMBO journal* **34**, 2465-2480 (2015).